Resonance Cases and Small Divisors in a Third Integral of Motion. II

GEORGE CONTOPOULOS AND MICHAEL MOUTSOULAS

Institute for Space Studies, Goddard Space Flight Center, National Aeronautics and Space Administration, New York, New York, and Thessaloniki University, Thessaloniki, Greece

(Received 20 September 1965)

This paper contains a complete description of the resonance case $A=B$, i.e., when the unperturbed frequencies in two perpendicular directions are equal. The form of the third integral is different from that of the nonresonance case. The secular terms are eliminated, step by step, and higher-order terms are calculated by means of a computer. The third integral is better conserved in actual orbits when more higher-order terms are included in it. The invariant curves give the main characteristics of the orbits. The theoretical invariant curves represent sufficiently well the empirically found invariant curves (by means of orbital calculations) when terms up to the fourth degree in the perturbation parameter ϵ are included. A complete classification of the orbits can be achieved even by using the zero-order terms of the third integral. For accurate numerical results, however, we need to include terms up to the second or even to the fourth order, especially in the case that ϵ approaches the value for which the curve of zero velocity opens and the moving point may go to infinity.

There are three main types of orbits: the A-, B-, and C-type orbits. Their boundaries are calculated numerically and some characteristic points are found by means of the third integral numerically or by series expansions. A detailed comparison between theory and numerical experiments gives always good agreement when sufficient terms of the third integral are included. Five periodic orbits have been found, three stable and two unstable. The transition types have also been discussed in detail.

These calculations are applied to the galactic orbits on the plane of symmetry of a distorted (nonaxisymmetric) galaxy. If the distortion is of the order of 20%, we find that the circular orbits become almost rectilinear through the central region and then reverse the sense of rotation in a few billion years.

A second application refers to the energy exchange between two coupled oscillators. The third integral predicts the correct amount of energy exchange. In one case the energy of one of the oscillators varies between 0 and $\frac{2}{3}$ of the total energy.

I. CASE $A=B$. THE "THIRD" INTEGRAL

IN this paper we apply the methods developed in paper I (Contopoulos 1963) in the case $A=B$.

A change of notations is introduced, because we are dealing now with two-dimensional fields, that have no connection with the three-dimensional galactic potential, for which the third integral was derived first (Contopoulos 1960). Therefore, we introduce coordinates x, y instead of ξ, z, velocities X, Y, instead of R, Z, constants A, B, ϵ, c_1, c_2, c_3 instead of P, Q, b, x_1, x_2, x_3, and the functions H, Φ_1, Φ_2, Φ_{10}, Φ_{20}, etc., instead of F, Φ, V, Φ_0, V_0, etc.

The potential field is now

$$V=\tfrac{1}{2}(Ax^2+By^2)-\epsilon xy^2, \tag{1}$$

and $A=B$. The zero-order term of the third integral is

$$\varphi_0=c_1(2\Phi_{10})^2+c_2(2\Phi_{10})(2\Phi_{20})+c_3(2\Phi_{20})^2+C_0, \tag{2}$$

where c_1, c_2, c_3 are constants to be defined later,

$$2\Phi_{10}=X^2+Ax^2, \tag{3}$$

$$2\Phi_{20}=Y^2+Ay^2, \tag{4}$$

$$C_0=(2\Phi_{10})(2\Phi_{20})\cos 2A^{\frac{1}{2}}T_0, \tag{5}$$

and T_0 is given through the equations

$$x=\frac{(2\Phi_{10})^{\frac{1}{2}}}{A^{\frac{1}{2}}}\sin A^{\frac{1}{2}}(T-T_0), \quad y=\frac{(2\Phi_{20})^{\frac{1}{2}}}{A^{\frac{1}{2}}}\sin A^{\frac{1}{2}}T,$$
$$X=(2\Phi_{10})^{\frac{1}{2}}\cos A^{\frac{1}{2}}(T-T_0), \quad Y=(2\Phi_{20})^{\frac{1}{2}}\cos A^{\frac{1}{2}}T; \tag{6}$$

hence

$$C_0=X^2Y^2-Ax^2Y^2-AX^2y^2+A^2x^2y^2+4AxXyY. \tag{7}$$

We also have the energy integral

$$H=H_0+\epsilon H_1=\tfrac{1}{2}(Ax^2+X^2+Ay^2+Y^2)-\epsilon xy^2=h, \tag{8}$$

where $H_0=\Phi_{10}+\Phi_{20}$, $H_1=-xy^2$, and h is the total energy.

It is easy to show that if we multiply the term Φ_2 (Contopoulos 1960) by $-(2B/3)(4B-A)(A-B)$ and then set $A\rightarrow B$, we get the limit C_0. We therefore take the integral

$$\varphi_0=\varphi_0+\epsilon\varphi_1+\epsilon^2\varphi_2+\cdots, \tag{9}$$

and we calculate c_1, c_2, c_3 so that φ_2 shall not have secular terms.

The higher-order terms are given through the recurrent formula

$$\varphi_{\nu+1}=-\int(\varphi_\nu,H_1)dT+f(\Phi_{10},\Phi_{20},T_0), \tag{10}$$

where

$$(\varphi_\nu,H_1)=(\partial\varphi_\nu/\partial X)y^2+(\partial\varphi_\nu/\partial Y)2xy, \tag{11}$$

and f is an arbitrary function of Φ_{10}, Φ_{20}, T_0, which is a polynomial in x, X, y, Y. Then we find

$$\varphi_1=\bar{C}_1+4c_1\Phi_{11}(2\Phi_{10})+2c_2[\Phi_{11}(2\Phi_{20})+\Phi_{21}(2\Phi_{10})]+4c_3\Phi_{21}(2\Phi_{20}), \tag{12}$$

where

$$\bar{C}_1=-\frac{2A}{3}\Big\{2x^3y^2-\frac{6}{A^2}(AxX^2y^2-xX^2Y^2+X^3yY)+\frac{2x^3Y^2}{A}+\frac{6x^2XyY}{A}+xy^4-\frac{3xy^2Y^2}{A}-\frac{2}{A^2}(xY^4-XyY^3)+\frac{4}{A}Xy^3Y\Big\}, \quad (13)$$

$$\Phi_{11}=-(1/3A)(Axy^2+2xY^2-2XyY), \quad (14)$$

and

$$\Phi_{21}=H_1-\Phi_{11}; \quad (15)$$

$\bar{C}_1$ has been found from C_0 in the same way as Φ_{11} is found from Φ_{10}.

If we calculate now φ_2 we find the following secular terms:

$$-\frac{4\bar{A}+\bar{B}}{6A^{2\frac{1}{2}}}+c_1\left(-\frac{2\bar{A}}{A^{2\frac{1}{2}}}\right)+c_2\left(\frac{\bar{A}-\bar{B}}{A^{2\frac{1}{2}}}\right)+c_3\left(\frac{2\bar{B}}{A^{2\frac{1}{2}}}\right), \quad (16)$$

where

$$\bar{A}=T(2\Phi_{10})^2(2\Phi_{20})\sin 2A^{\frac{1}{2}}T_0,$$
$$\bar{B}=T(2\Phi_{10})(2\Phi_{20})^2\sin 2A^{\frac{1}{2}}T_0. \quad (17)$$

The terms (16) must be zero, therefore

$$2+6c_1-3c_2=0 \quad \text{and} \quad 1+6c_2-12c_3=0. \quad (18)$$

One solution of this system is

$$c_{10}=-\tfrac{1}{3}, \quad c_{20}=0, \quad c_{30}=+\tfrac{1}{12}. \quad (19)$$

All other solutions are

$$c_1=c_{10}+c_1', \quad c_2=c_{20}+c_2', \quad c_3=c_{30}+c_3', \quad (20)$$

where

$$c_1'=\tfrac{1}{2}c_2'=c_3', \quad (21)$$

in agreement with the general theory developed in paper I.

Therefore the integral (9) is written

$$\varphi=\varphi_0+\epsilon\varphi_1+\cdots=X^2Y^2-Ax^2Y^2-AX^2y^2+A^2x^2y^2+4AxXyY-\frac{(2\Phi_{10})^2}{3}+\frac{(2\Phi_{20})^2}{12}-\frac{2\epsilon}{9A}(4A^2xy^4+4A^2x^3y^2+2Ax^3Y^2+22Ax^2XyY-20AxX^2y^2+14xX^2Y^2-14X^3yY+13AXy^3Y-7xY^4+7XyY^3-9Axy^2Y^2)+\cdots=\varphi_{;0}=\varphi_{0;0}+\epsilon\varphi_{1;0}+\cdots, \quad (22)$$

where the zero after the semicolon means that φ, φ_0, $\varphi_1\cdots$ are calculated for $x=x_0$, $X=X_0$, $y=y_0$, $Y=Y_0$.

If we calculate higher-order terms by means of a computer (details will be given in another paper) we find that φ_2 has no secular terms and φ_4 has the secular terms

$$T(2\Phi_{10})(2\Phi_{20})\Big[-\frac{6.875}{27A^{5\frac{1}{2}}}(2\Phi_{10})^2-\frac{36.5}{9A^{5\frac{1}{2}}}(2\Phi_{10})(2\Phi_{20})+\frac{98.28125}{27A^{5\frac{1}{2}}}(2\Phi_{20})^2\Big]\sin 2A^{\frac{1}{2}}T_0-T(2\Phi_{10})^2(2\Phi_{20})^2\times\frac{13.9375}{9A^{5\frac{1}{2}}}\sin 4A^{\frac{1}{2}}T_0. \quad (23)$$

If we add in φ_2 the terms

$$\bar{c}_1(2\Phi_{10})^3+\bar{c}_2(2\Phi_{10})^2(2\Phi_{20})+\bar{c}_3(2\Phi_{10})(2\Phi_{20})^2+\bar{c}_4(2\Phi_{20})^2+[d_1(2\Phi_{10})+d_2(2\Phi_{20})]\varphi_0, \quad (24)$$

where $\varphi_0=C_0-\frac{1}{3}(2\Phi_{10})^2+\frac{1}{12}(2\Phi_{20})^2$, we find also the following secular terms in φ_4:

$$Tq\Big\{\Big(6\bar{c}_1-2\bar{c}_2-\frac{2d_1}{3}+\frac{2d_2}{3}\Big)(2\Phi_{10})^2+(4\bar{c}_2-4\bar{c}_3)(2\Phi_{10})(2\Phi_{20})+\Big(2\bar{c}_3-6\bar{c}_4+\frac{d_1}{6}-\frac{d_2}{6}\Big)(2\Phi_{20})^2\Big\}\times(2\Phi_{10})(2\Phi_{20})\sin 2A^{\frac{1}{2}}T_0+Tq(d_1-d_2)(2\Phi_{10})^2(2\Phi_{20})^2\times\sin 4A^{\frac{1}{2}}T_0. \quad (25)$$

where $q(=-1/2A^{2\frac{1}{2}})$ is the coefficient of the secular term $T(2\Phi_{10})(2\Phi_{10})\sin 2A^{\frac{1}{2}}T_0$, appearing in the term Φ_{12} of the expansion Φ_1.

The last term of (25) is essentially the secular term of $d_1(2\Phi_{10})+d_2(2\Phi_{20})$, which is $T(2q)(d_1-d_2)(2\Phi_{10})(2\Phi_{20})\times\sin 2A^{\frac{1}{2}}T_0$, multiplied by $C_0=(2\Phi_{10})(2\Phi_{20})\cos 2A^{\frac{1}{2}}T_0$.

In order that the totality of secular terms should vanish we must have

$$-3\bar{c}_1+\bar{c}_2+\frac{d_1}{3}-\frac{d_2}{3}-\frac{6.875}{27A^3}=0,$$
$$-2\bar{c}_2+2\bar{c}_3-\frac{36.5}{9A^3}=0, \quad (26)$$
$$-\bar{c}_3+3\bar{c}_4-\frac{d_1}{12}+\frac{d_2}{12}+\frac{98.28125}{27A^3}=0,$$
$$-\frac{d_1}{2}+\frac{d_2}{2}-\frac{13.9375}{9A^3}=0.$$

The solution of this system is

$$d_1=-(27.875/9A^3)+d_2,$$
$$\bar{c}_2=-(18.25/9A^3)+\bar{c}_3, \quad (27)$$
$$\bar{c}_4=-(105.25/81A^3)+\tfrac{1}{3}\bar{c}_3,$$
$$\bar{c}_1=-(89.5/81A^3)+\tfrac{1}{3}\bar{c}_3,$$

where $\bar{c}_3$, d_2 are arbitrary. However, the terms with $\bar{c}_3$ and d_2 are now

$$\tfrac{1}{3}\bar{c}_3(2H_0)^3+d_2(2H_0)\varphi_0,$$

i.e., they are combinations of the integrals H_0 and φ_0, that are used presently; thus we may set $\bar{c}_3 = d_2 = 0$. Then the terms of 6th, 7th, and 8th degree, as given by the computer, are:

φ_2 (total)					
6	0	0	0	6	−0.151466049382716 E 04
6	0	0	2	4	−0.454398148148148 E 04
6	0	0	4	2	−0.415509259259259 E 04
6	0	0	6	0	−0.903549382716049 E 03
6	0	2	0	4	+0.325231481481481 E 03
6	0	2	2	2	+0.259490740740740 E 04
6	0	2	4	0	−0.239699074074074 E 04
6	0	4	0	2	−0.598611111111111 E 04
6	0	4	2	0	+0.198611111111111 E 04
6	0	6	0	0	−0.725308641975308 E 02
6	1	1	1	3	−0.388888888888888 E 04
6	1	1	3	1	+0.544444444444444 E 04
6	1	3	1	1	−0.159444444444444 E 05
6	2	0	0	4	+0.226967592592592 E 04
6	2	0	2	2	−0.362731481481481 E 04
6	2	0	4	0	−0.123032407407407 E 04
6	2	2	0	2	−0.400000000000000 E 04
6	2	2	2	0	−0.711111111111111 E 04
6	2	4	0	0	−0.217592592592592 E 03
6	3	1	1	1	−0.972222222222222 E 04
6	4	0	0	2	+0.430555555555555 E 03
6	4	0	2	0	−0.354166666666666 E 04
6	4	2	0	0	−0.217592592592592 E 03
6	6	0	0	0	−0.725308641975308 E 02
φ_3					
7	0	1	1	5	0.126129982106037 E 06
7	0	1	3	3	0.212672932762558 E 06
7	0	1	5	1	0.261083109288592 E 05
7	0	3	1	3	−0.105194532781774 E 06
7	0	3	3	1	0.253314056765462 E 06
7	0	5	1	1	−0.294130862860600 E 06
7	1	0	0	6	−0.126129982106036 E 06
7	1	0	2	4	−0.279383327229380 E 05
7	1	0	4	2	0.343360889150380 E 06
7	1	0	6	0	0.177707316350357 E 06
7	1	2	0	4	0.105194532781773 E 06
7	1	2	2	2	−0.318335951123616 E 06
7	1	2	4	0	0.208866487430890 E 04
7	1	4	0	2	0.294130862860601 E 06
7	1	4	2	0	−0.280369098969127 E 06
7	2	1	1	3	0.329794327583611 E 06
7	2	1	3	1	0.649652856839897 E 06
7	2	3	1	1	0.217767713437275 E 06
7	3	0	0	4	−0.398017540066871 E 05
7	3	0	2	2	−0.201800163276670 E 06
7	3	0	4	0	0.253079813975820 E 06
φ_3					
7	3	2	0	2	0.319585246001708 E 06
7	3	2	2	0	0.440766849176554 E 05
7	4	1	1	1	0.427571172026716 E 06
7	5	0	0	2	0.423198639953398 E 05
7	5	0	2	0	0.228874725712803 E 06
φ_4					
8	0	0	0	8	0.243407600308641 E 06
8	0	0	2	6	0.973630401234566 E 06
8	0	0	4	4	0.463300540123455 E 06
8	0	0	6	2	−0.812017746913580 E 06
8	0	0	8	0	−0.306206597222221 E 06
8	0	2	0	6	0.283143325617282 E 07
8	0	2	2	4	0.165508294753085 E 07
8	0	2	4	2	0.517759452160490 E 07
8	0	2	6	0	−0.414265046296280 E 06
8	0	4	0	4	0.162914737654321 E 07
8	0	4	2	2	−0.902874228395068 E 07
8	0	4	4	0	0.594103009259262 E 07
8	0	6	0	2	0.251963734567901 E 07
8	0	6	2	0	−0.266886574074075 E 07
8	1	1	1	5	0.136784336419752 E 08
8	1	1	3	3	−0.411041666666666 E 07
8	1	1	5	1	−0.111907021604938 E 08
8	1	3	1	3	0.245740740740740 E 08
8	1	3	3	1	0.468456790123452 E 07
8	1	5	1	1	0.103770061728395 E 08
8	2	0	0	6	−0.400778356481483 E 07
8	2	0	2	4	0.187473476080246 E 08
8	2	0	4	2	0.168794656635802 E 08
8	2	0	6	0	−0.690128279320986 E 07
8	2	2	0	4	−0.902874228395061 E 07
8	2	2	2	2	0.315393518518520 E 07
8	2	2	4	0	0.239459490740740 E 08
8	2	4	0	2	0.237040895061728 E 07
8	2	4	2	0	0.648314043209876 E 07
8	3	1	1	3	0.156234567901244 E 07
8	3	1	3	1	−0.186049382716050 E 08
8	3	3	1	1	0.215154320987651 E 07
8	4	0	0	4	−0.490495756172841 E 07
8	4	0	2	2	−0.399417438271600 E 07
8	4	0	4	0	−0.364708719135801 E 07
8	4	2	0	2	0.183252314814815 E 07
8	4	2	2	0	0.357781635802467 E 07
8	5	1	1	1	−0.749212962962965 E 07
8	6	0	0	2	0.185952932098766 E 07
8	6	0	2	0	−0.456307870370370 E 07

The first integer indicates the degree of the term, the next four integers are the exponents of $(A^{\frac{1}{2}}x)$, X, $(A^{\frac{1}{2}}y)$, Y, and the last number is the coefficient of the term; its last figure may be in error by one unit.

The terms of 8th degree are given before any correction to eliminate the secular terms of degree 10. The additional terms are functions of Φ_{10}, Φ_{20}, and φ_0; their effect is of the same form as that of the terms discussed above, but smaller because of the factor ϵ^4. For all practical applications the terms written provide roughly accurate results.

In order to check the accuracy of the third integral a number of orbits were calculated numerically, by means of the Runge–Kutta method in double precision. The energy constant along the orbits was checked to be constant, up to the limit of the eight printed significant figures. In many points of each orbit the third integral was calculated, truncated after the term φ_0,

TABLE I. Accuracy of the third integral.

	φ_0			φ_1			φ_2			φ_3			φ_4		
	M	m	D	M	m	D	M	m	D	M	m	D	M	m	D
a''	.206	.144	.06	.195	.182	.013	.175	.173	.002	.17352	.17341	.00011	.17347	.17343	.00004
a'	.21	.01	.20	.20	.12	.08	.078	.026	.052	.065	.059	.006	.062	.060	.002
b'	.32	.07	.25	.24	.16	.08	.130	.076	.054	.115	.108	.007	.111	.109	.002
c'	−.80	−.93	.13	−.859	−.866	.007	−.854	−.858	.004	−.8553	−.8560	.0007	−.8555	−.8557	.0002
a	.2	−.5	.7	.20	−.20	.40	−.19	−.65	.46	−.21	−.35	.14	−.26	−.33	.07
b	.4	−.2	.6	.31	−.01	.32	−.06	−.64	.58	−.01	−.20	.19	−.13	−.18	.05
c	.4	−.2	.6	.36	−.02	.38	−.05	−.66	.61	−.02	.18	.20	−.13	−.17	.04
d	−.4	−1.4	1.7	.52	.32	.20	.32	−.42	.74	.70	.22	.48	.32	.23	.09
e	.4	−.2	.6	.34	.09	.25	−.02	−.66	.64	−.03	−.18	.15	−.10	−.16	.06
f	.4	−.2	.6	.36	−.00	.36	−.05	−.66	.61	−.06	−.21	.15	−.12	−.19	.07
g	−.6	−1.0	.4	−.76	−.82	.06	−.78	−.83	.05	−.793	−.806	.013	−.796	−.806	.010
h	−.7	−1.0	.3	−.84	−.91	.07	−.83	−.86	.03	−.829	−.841	.012	−.831	−.840	.009

Units 10^{-4}.

$\epsilon\varphi_1$, $\epsilon^2\varphi_2$, $\epsilon^3\varphi_3$, and $\epsilon^4\varphi_4$. In Table I we give the maximum M and minimum m value of the integral and the difference $D=M-m$.

If we calculate the relative error of the third integral $2D/|M+m|$ we find:

(a) In the case a'', when the perturbation is small ($\epsilon=0.02$), the relative error is about 0.07 if the third integral is truncated after $\epsilon\varphi_1$, 0.01 after $\epsilon^2\varphi_2$, 0.0006 after $\epsilon^2\varphi_3$, and 0.0002 after $\epsilon^4\varphi_4$.

(b) When the perturbation is intermediate, in cases a' and b', ($\epsilon=0.05$) the relative error is about 0.4–1.0 if the third integral is truncated after $\epsilon\varphi_1$ or $\epsilon^2\varphi_2$, about 0.1 after $\epsilon^3\varphi_3$, and about 0.02–0.03 after $\epsilon^4\varphi_4$. In case c' ($\epsilon=0.05$) the accuracy is almost 100 times better; the relative error is only about 0.0002 after $\epsilon^4\varphi_4$.

(c) When the perturbation is large ($\epsilon=0.1$) the accuracy is small. The relative error, when terms up to $\epsilon^3\varphi_3$ are included is of order 1, except in cases g, h, when it is of order 0.01–0.02. After $\epsilon^4\varphi_4$ the relative error becomes 0.2–0.5; in cases g, h it is of order 0.01.

Therefore the truncated third integral is accurate enough for small perturbations, but rather poorly conserved when the perturbation is large. The case $\epsilon=0.1$ is near the escape case ($\epsilon=0.118$), when the curve of zero velocity opens and the moving point may go to infinity.

It is important, however, to note that even in this case the third integral is better conserved when the number of terms increases. When the terms $\epsilon^4\varphi_4$ are included this integral begins to be approximately constant. Therefore in order to apply theoretical results to actual orbits the inclusion of terms up to $\epsilon^4\varphi_4$ is necessary. This is done below in a few cases. In general, however, only zero-order results are given. It is remarkable, therefore, that the orbits are very similar, topologically, to the zero-order results found below.

It is also to be noted that the third integral is much better conserved for orbits of type C (Sec. III), i.e., orbits that fill a ring around the origin, and orbits with initial conditions near those of type C (orbits c', h, and g).

II. INVARIANT CURVES

If we eliminate Y between Eqs. (8) and (22) we find the projection of the section of the third integral supersurface by the energy integral supersurface on the xyX space.

This is a surface on which lie the projections of the orbits in the three-dimensional space xyX (called hereafter simply orbits), whose initial points lie on it.

The section of this surface by the plane $y=0$ is a curve which contains the points of intersection of the orbits by the same plane. Such curves are called invariant curves (Contopoulos 1965); their form gives many indications about the general properties of the orbits.

The equation of an invariant curve going through the point (x_0,X_0), when the energy is

$$h=\tfrac{1}{2}(Ax_0^2+X_0^2+Y_0^2), \tag{28}$$

is found if we put $y=0$ and $Y^2=2h-Ax^2-X^2$ in Eq. (22), namely

$$15X^4-2X^2(10h-3Ax^2)-9A^2x^4+28hAx^2 + (8\epsilon x/3A)(2h-X^2-Ax^2)(21X^2+9Ax^2-14h)+\cdots = \text{the same function at the initial point.} \tag{29}$$

The invariant curves are always inside the "limiting curve"

$$X^2+Ax^2=2h, \tag{30}$$

which is a circle in the $A^{\frac{1}{2}}x$, X plane.

Equation (29) is written in zero order

$$\theta(Ax^2,X^2)=15X^4-2X^2(10h-3Ax^2) -9A^2x^4+28hAx^2-15X_0^4+2X_0^2(10h-3Ax_0^2) +9A^2x_0^4-28hAx_0^2=0. \tag{31}$$

In order to have real solutions for X^2 we must have

$$\mathcal{J}(Ax^2)=144A^2x^4-480hAx^2+100h^2+225X_0^4 -30X_0^2(10h-3Ax_0^2)-135A^2x_0^4+420hAx_0^2\geq 0. \tag{32}$$

Further the solution must be between 0 and $2h-Ax^2$.

But

$$\theta(Ax^2,0)=-9A^2x^4+28hAx^2-15X_0^4+2X_0^2(10h-3Ax_0)^2 +9A^2x_0^4-28hAx_0^2, \quad (33)$$

and

$$\theta(Ax^2,\ 2h-Ax^2) =(10h+15X_0^2-9Ax_0^2)Y_0^2=\theta(0,2h). \quad (34)$$

Hence if

$$10h+15X_0^2-9Ax_0^2<0 \quad (35)$$

we have one solution for X^2 acceptable, if $(A^{\frac{1}{2}}x_0,X_0)$ is inside the "limiting curve" (case C). In Fig. 1 the regions C are to the right and left of the two branches of the hyperbola

$$10h=9Ax^2-15X^2, \quad (36)$$

which intersects the axis $A^{\frac{1}{2}}x$ at the points $[A^{\frac{1}{2}}x=\pm(10h/9)^{\frac{1}{2}}, X=0]$, and the limiting curve at the points $[A^{\frac{1}{2}}x=\pm(5h/3)^{\frac{1}{2}}, X=\pm(h/3)^{\frac{1}{2}}]$. In case C we have always $\mathcal{J}(Ax^2)>0$, because the discriminant of $\mathcal{J}(Ax^2)$ is negative.

Further we must have

$$\theta(Ax^2,0)\geqslant 0. \quad (37)$$

The equation $\theta(Ax^2,0)=0$ has two real roots

$$Ax_i^2=\frac{14h}{9}\pm\tfrac{1}{9}\{[14h-9(X_0^2+Ax_0^2)]^2 +216X_0^2(2h-X_0^2-Ax_0^2)\}^{\frac{1}{2}}, \quad (38)$$

which coincide only if $X_0^2=0$ and $Ax_0^2=14h/9$. Thus

$$\theta(Ax^2,0)=9(Ax_2^2-Ax^2)(Ax^2-Ax_1^2). \quad (39)$$

The invariant curves are small closed curves around the points P_3, $P_4[A^{\frac{1}{2}}x=\pm(14h/9)^{\frac{1}{2}}, X=0]$ in Fig. 1. The corresponding orbits surround the stable periodic orbits corresponding to the points P_3, P_4 (see Sec. IV).

If

$$10h+15X_0^2-9Ax_0^2>0 \quad (40)$$

then $\mathcal{J}(Ax^2)$ has two real roots Ax_b^2, $Ax_a^2(x_b^2\geqslant x_a^2)$. The mean of the roots is $5h/3$, hence $Ax_a^2<5h/3$. In order that $\mathcal{J}(Ax^2)$ should be positive, we must have $x^2\leq x_a^2$, or $x^2\geqslant x_b^2$. The latter case does not occur inside the "limiting curve" if inequality (40) is satisfied, because then the maximum value of Ax^2 is $5h/3$. Thus $|x_a|$ is the maximum value of $|x|$.

The mean of the roots of Eq. (31) is $(10h-3Ax^2)/15$, which is between 0 and $2h-Ax^2$. Further $\theta(Ax^2,\ 2h-Ax^2)>0$; therefore if $\theta(Ax^2,0)>0$ there are two acceptable roots and if $\theta(Ax^2,0)<0$ there is one acceptable root.

If $Ax_1^2<0$, then for $0<Ax^2<Ax_a^2$ we have two acceptable roots for X^2 (case B).

If $Ax_1^2>0$, then for $0<Ax^2<Ax_1^2$ we have one acceptable root and for $Ax_1^2<Ax^2<Ax_a^2$ two acceptable roots for X^2 (case A).

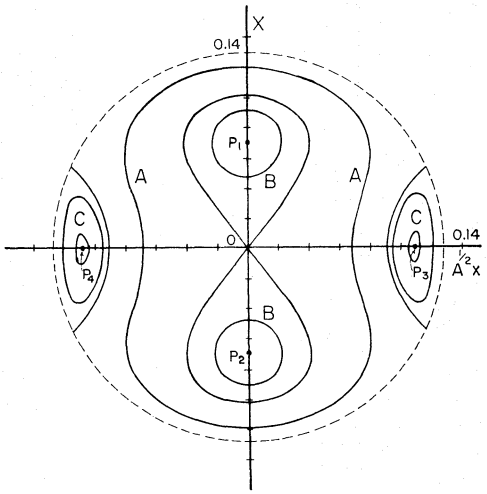

FIG. 1. Theoretical curves in the plane $A^{\frac{1}{2}}x$, X for $A=0.1$, $2h=0.0153$, $\epsilon\to 0$. The dashed line is the limiting curve $Ax^2+X^2=2h$ (circle).

The transition case between cases A and B happens if $x_1^2=0$, or

$$\theta(0,0)=-15X_0^4+2X_0^2(10h-3Ax_0^2) +9Ax_0^4-28hAx_0^2=0. \quad (41)$$

This equation represents a figure eight curve going through the origin 0. Its sections by the axis X are $X_0=0$ and $X_0=\pm(4h/3)^{\frac{1}{2}}$.

We have always $Ax_a^2>Ax_1^2$, because for $Ax^2=Ax_a^2$ Eq. (31) has a double root

$$X^2=(10h-3Ax_a^2)/15\neq 0,$$

hence $\theta(Ax_a^2,0)>0$; therefore, according to Eq. (39), Ax_0^2 is between the roots Ax_1^2, Ax_2^2.

If $Ax_a^2=0$, then we must have $Ax^2=0$ and Eq. (31) has a double root $X^2=2h/3$. We have also

$$\theta(0,\tfrac{2}{3}h)\equiv-\tfrac{1}{3}[5(2h-3X_0^2-Ax_0^2)^2 +4Ax_0^2(26h-3X_0^2-8Ax_0^2)]=0, \quad (42)$$

therefore $Ax_0^2=0$ and $X_0^2=\frac{2}{3}h$.

Hence the invariant curves in case B surround the points P_1, $P_2[x_0=0, X_0=\pm(\frac{2}{3}h)^{\frac{1}{2}}]$ (Fig. 1), which represent stable periodic orbits. The invariant curves near the periodic ones represent "tube" orbits (see Sec. IV).

We see that the invariant curves permit immediately the classification of the different forms of orbits.

The above discussion has been made for $\epsilon\to 0$. For ϵ finite the invariant curves are somehow distorted. The main types of orbits are, however, the same.

Figure 1 gives the invariant curves, when $\epsilon\to 0$. If $\epsilon\neq 0$ higher-order terms of the third integral must be taken also in consideration. Figure 2 (a), (b), gives the invariant curves when $\epsilon=0.1$ $(=A)$, $2h=0.0153$, and the third integral is truncated after the terms $\epsilon^2\varphi_2$ (a), or $\epsilon^4\varphi_4(b)$. Their form is progressively changed as

higher-order terms are included, but the general succession of A, B, C type orbits is the same.

Figure 3 represents the actual invariant curves, i.e., the locus of the points $(A^{\frac{1}{2}}x,X)$ when $y=0$ along a number of orbits calculated numerically. It is seen that the curves of Fig. 2(b) are very near the corresponding invariant curves of Fig. 3. Of course, the agreement is even better for smaller values of ϵ.

III. THE BOUNDARIES OF THE ORBITS

In order to find theoretically the boundary of an orbit in the x y plane, we have to eliminate X and Y between Eqs. (8), (22) and

$$J=\frac{\partial\varphi}{\partial X}Y-\frac{\partial\varphi}{\partial Y}X=0, \tag{43}$$

or

$$J=XY\left\{2(Y^2-X^2)+2A(x^2-y^2)-4\left(\frac{X^2+Ax^2}{3}\right)-\left(\frac{Y^2+Ay^2}{3}\right)-\frac{4\epsilon x}{9A}[-2Ax^2-20Ay^2-14(X^2-Y^2)+14Y^2+9Ay^2]\right\}$$
$$-4Axy(X^2-Y^2)-\frac{2\epsilon y}{9A}[-22Ax^2(X^2-Y^2)-14(3X^2Y^2-X^4)-13Ay^2(X^2-Y^2)+7(Y^4-3X^2Y^2)]+\cdots=0. \tag{44}$$

We first find the boundary in zero order, omitting all terms with ϵ in the equations.

The energy integral gives

$$X^2=C_1-Y^2, \tag{45}$$

where

$$C_1=2h-A(x^2+y^2). \tag{46}$$

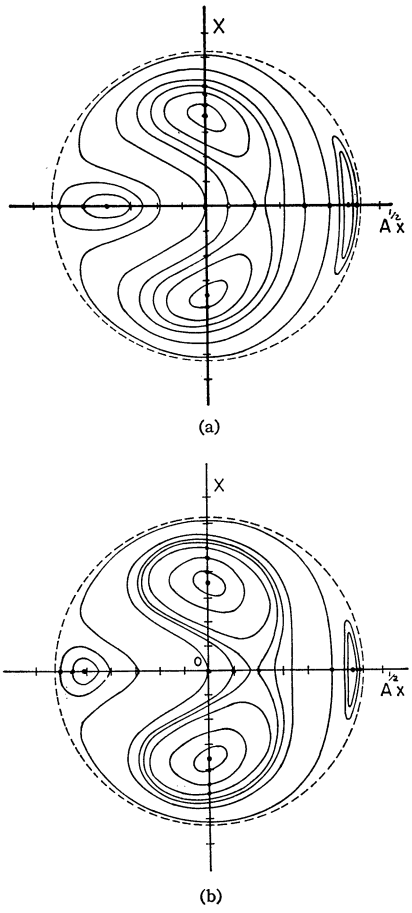

FIG. 2. Theoretical invariant curves for $\epsilon=A=0.1$, $2h=0.0153$. (a) The third integral is truncated after $\epsilon^2\varphi_2$. (b) The third integral is truncated after $\epsilon^4\varphi_4$. The initial points are marked by dots.

If we insert this value into the zero-order terms of Eq. (22) we find

$$48Axy\,XY=15Y^4-2C_2Y^2+C_3, \tag{47}$$

where

$$C_2=20h-3A(4x^2+y^2), \tag{48}$$

and

$$C_3=16h^2+8hAy^2-3A^2y^2(8x^2+3y^2)+12\varphi_{0;0}. \tag{49}$$

The zero-order terms of Eq. (44) are written, by means of Eq. (45),

$$XY(-15Y^2+C_2)=12Axy(2Y^2-C_1). \tag{50}$$

We have to eliminate X and Y between Eqs. (45), (47), and (50).

By eliminating the product XY between Eqs. (47) and (50), we find

$$225Y^6-45C_2Y^4+C_4Y^2-C_5=0, \tag{51}$$

where

$$C_4=2C_2^2+15C_3+1152A^2x^2y^2, \tag{52}$$

and

$$C_5=C_2C_3+576A^2x^2y^2C_1. \tag{53}$$

Raising both members of Eq. (47) to the square and using again Eq. (45) we find

$$225Y^8-60C_2Y^6+2C_4Y^4-4C_5Y^2+C_3^2=0. \tag{54}$$

We eliminate Y^2 between Eqs. (51) and (54) as

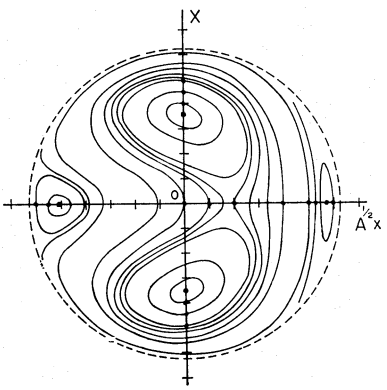

FIG. 3. Observed invariant curves for orbits calculated numerically for $\epsilon=A=0.1$, $2h=0.0153$. The initial points are marked by dots.

follows: We subtract Eq. (54) from Eq. (51) multiplied by Y^2 and find

$$15C_2Y^6-C_4Y^2+3C_5Y^2-C_3^2=0. \quad (55)$$

Then we multiply Eq. (51) by C_2 and subtract it from Eq. (55) multiplied by 15:

$$15(3C_2^2-C_4)Y^4+(45C_5-C_2C_4)Y^2 +C_2C_5-15C_3^2=0. \quad (56)$$

If we multiply now this equation by $15Y^2$ and subtract from it Eq. (51) multiplied by $(3C_2^2-C_4)$ we find

$$15(45C_5+9C_2^3-4C_2C_4)Y^4 +(15C_2C_5-225C_3^2-3C_2^2C_4+C_4^2)Y^2 +C_5(3C_2^2-C_4)=0. \quad (57)$$

Now we can easily eliminate Y^2 between the two second-order equations (56) and (57), and find

$$[15(3C_2^2-C_4)^2C_5-15(45C_5+9C_2^3-4C_2C_4)(C_2C_5-15C_3^2)]^2 =[(15C_2C_5-225C_3^2-3C_2^2C_4+C_4^2)(C_2C_5-15C_3^2)-(3C_3^2-C_4)C_5(45C_5-C_2C_4)] \times[15(45C_5-C_2C_4)(45C_5+9C_2^3-4C_2C_4)-15(15C_2C_5-225C_3^2-3C_2^2C_4+C_4^2)(3C_2^2-C_4)]. \quad (58)$$

This is the equation of the boundary in zero-order approximation. It has been solved with the help of the IBM 709 computer of the Yale University. Some of the results found this way are represented in Figs. 4(a)–(e).

In all cases almost the same energy was used, $h\simeq 0.00765$ and $A=0.1$. The angular points $C_1C_2C_3C_4$ are always on the curve of zero velocity, which is the circle $A(x^2+y^2)=2h$.

It is to be noted that Eq. (58), because it involves raising to the square of Eq. (47), gives also spurious solutions that do not correspond to the real boundary. This can be checked in the case of special points (subsections A–E below). In Figs. 4 we include only the real boundaries of the orbits in zero-order approximation.

Figure 4(a) represents the boundary of an orbit of type A ("hour glass" orbit). The boundary has four angular points on the curve of zero velocity C_1, C_2, C_3, C_4 and leaves four open spaces inside it. The boundaries b_1, b_2, b_3, b_4 are extended inwards and there are also two branches d_1, d_2 perpendicular to the x axis. The inner boundaries are defined as envelopes of sets of partial arcs of the orbits. All these characteristics are present in the actual orbits [Figs. 5(a'',a',a,b,f,g)].

Figure 4(b) represents another boundary of a type A orbit.

Figure 4(c) represents the boundary of an orbit of type B ("tube" orbit). The angular points on the curve of zero velocity and the four open spaces are now quite different [cf. Figs. 5(b',c,d,e)].

The transition between type A and type B orbits is shown in Fig. 4(d). Two symmetric orbits of type B (namely $C_1C_2'C_3C_4'$ and $C_2C_2'C_4C_4'$) combine into one. The arcs C_1C_2, C_3C_4 are tangent to the curve of zero velocity at the points C_2', C_4'. The y axis is an unstable periodic orbit. The arcs C_4C_2' and C_3C_2' are tangent to each other at the point C_2' and the arcs C_1C_4', C_2C_4' at the point C_4'.

The actual transition form, when $\epsilon\neq 0$, is shown in Fig. 6.

Figure 4(e) represents the boundary of a type C orbit ("shell" orbit), which does not have points in common with the curve of zero velocity [cf. Figs. 5(c',h)].

The transition form between type A and type C orbits is shown in Fig. 6.

Some special points of the boundary can be found directly in zero and first-order approximation from Eqs. (8), (22), and (44). Because of the form of the equations of motion every orbit crosses the x axis, therefore we assume $y_0=0$.

A. Section with the Curve of Zero Velocity

If $C_1=0$ we have $X=Y=0$ and Eq. (47) gives $C_3=0$. Inserting the value $By^2=2h-Bx^2$ in $C_3=0$ we find

$$C(Ax^2)=15A^2x^4-20hBx^2-4h^2+12\varphi_{0;0}=0. \quad (59)$$

The solutions of this equation for Ax^2 are always real because the discriminant is

$$20(32^2-36\varphi_{0;0}) =20[5(2X_0^2-Y_0^2)^2+5A^2(2x_0^2-y_0^2)^2 +52A(x_0Y_0-X_0y_0)^2+10A(2x_0X_0-y_0Y_0)^2]\geqslant 0. \quad (60)$$

This quantity is zero only if

$$2X_0^2=Y_0^2, \quad 2x_0^2=y_0^2, \quad x_0Y_0=X_0y_0 \quad \text{and} \quad 2X_0x_0=y_0Y_0.$$

These conditions are satisfied if and only if

$$y_0/x_0=Y_0/X_0=\pm\sqrt{2}.$$

Then the solution of Eq. (54) is

$$Ax^2=2h/3, \quad \text{hence} \quad Ay^2=4h/3, \quad \text{i.e.,} \quad y/x=\pm\sqrt{2}.$$

The solutions $y/x=Y/X=\pm\sqrt{2}$ represent periodic orbits.

In fact if we set $x_0=y_0=0$, $Y_0^2=2X_0^2$, we find

$$\varphi_0=2(X^2+Ax^2)^2, \qquad \varphi_{0;0}=(2/9)(2h)^2, \quad (61)$$

$$\varphi_1=-(16x^3/3)(X^2+Ax^2), \qquad \varphi_{1;0}=0, \quad (62)$$

$$\varphi_2=\left\{\left[-\frac{10000}{9}+\bar{c}_1+2\bar{c}_2+4\bar{c}_3+8\bar{c}_4+2(d_1+2d_2)\right]\times(X^2+Ax^2)^3+\frac{32x^6}{9}\right\}, \tag{63}$$

$$\varphi_{2;0}=\left[-\frac{10000}{9}+\bar{c}_1+2\bar{c}_2+4\bar{c}_3+8\bar{c}_4+2(d_1+2d_2)\right](2h)^3,$$

and Eq. (8) gives

$$X^2+Ax^2=\tfrac{1}{3}(2h+4\epsilon x^3). \tag{64}$$

Therefore if we include all terms up to ϵ^2 we find

$$\varphi_0+\epsilon\varphi_1+\epsilon^2\varphi_2-\varphi_{0;0}-\epsilon\varphi_{1;0}-\epsilon^2\varphi_{2;0}=0. \tag{65}$$

Similarly if we write

$$J=J_0+\epsilon J_1+\epsilon^2 J_2+\cdots,$$

we find along the above orbit $J_0=J_1=0$, and

$$J_2=\pm\sqrt{2}[6(\bar{c}_1+\bar{c}_2-4\bar{c}_4)+4(d_1-d_2)]X^2(X^2+Ax^2)^2=0.$$

The relation $\bar{c}_1+\bar{c}_2-4\bar{c}_4+\frac{2}{3}(d_1-d_2)=0$ was used in order to check the accuracy of the higher-order terms given by the computer.

Thus the straight lines $y=\pm\sqrt{2}x$ are periodic orbits in second-order approximation, and presumably to all approximations. The empirically found periodic solutions were, in fact, straight lines forming an angle $\tan^{-1}\sqrt{2}=54°44'$ with the x axis (Fig. 6).

In order that the boundary should have points in common with the curve of zero velocity we must have one root Ax^2, at least, positive and smaller than $2h$.

We have

$$C(0)=-4h^2+12\varphi_{0;0}=\theta(0,0) \tag{66}$$

and

$$C(2h)=16h^2+12\varphi_{0;0}=\theta(0,2h)>C(0). \tag{67}$$

The mean of the two roots is $\frac{2}{3}h$, i.e., it is between 0 and $2h$.

If $C(0)>0$, then also $C(2h)>0$, i.e., both roots are acceptable (case B). If $C(2h)<0$, then also $C(0)<0$, i.e., no root is acceptable (case C). If $C(2h)>0, C(0)<0$ only one root is acceptable (case A). If $x_0=y_0=0$, then

$$\varphi_{0;0}=X_0^2Y_0^2-\tfrac{1}{3}X_0^4+\tfrac{1}{12}Y_0^4, \tag{68}$$

and Eq. (59) is written

$$15A^2x^4-10(X_0^2+Y_0^2)Ax^2+10X_0^2Y_0^2-5X_0^4=0. \tag{69}$$

Its solutions are

$$Ax_1^2=X_0^2 \text{ and } Ax_2^2=\tfrac{1}{3}(2Y_0^2-X_0^2)=\tfrac{1}{3}(4h-3X_0^2). \tag{70}$$

The corresponding values of Ay^2 are

$$Ay_1^2=Y_0^2 \text{ and } Ay_2^2=\tfrac{1}{3}(4X_0^2+Y_0^2)=\tfrac{1}{3}(8h-3Y_0^2). \tag{71}$$

Hence we have one acceptable solution if $X_0^2>4h/3$ (case A) and two acceptable solutions if $X_0^2<4h/3$ (case B).

If ϵ is not very small a higher-order approximation is required. For example, in the calculated orbits it was found that for $x_0=y_0=0$ and X_0 very small we have orbits of type A and not of type B, as the zero-order theory would require.

If we solve numerically the equation $\varphi=\varphi_{;0}$ for $X=Y=0$, $Ay^2=(2h-Ax^2)/(1-2\epsilon x/A)$, $x_0=y_0=0$, $Y_0^2=2h-X_0^2$ and different values of X_0 we find (if the integral is truncated after $\epsilon^4\varphi_4$) that the transition between type A and type B orbits for $\epsilon=0.1$ occurs near $X_0=0.026$. Empirically the transition is found between $X_0=0.026$ and $X_0=0.027$. The transition orbit is an unstable periodic orbit, intersecting the $A^{\frac{1}{2}}x$ axis near $A^{\frac{1}{2}}x=0.037$. The corresponding invariant curve is a figure eight near the invariant curve going through $A^{\frac{1}{2}}x_0=0.04$ in Fig. 3.

The unstable periodic orbit is represented in Fig. 6, together with the boundary of an orbit of type A, whose initial conditions differ very little from those of the periodic orbit.

An inspection of Figs. 2(b) and 3 gives a transition invariant curve for $A^{\frac{1}{2}}x_0=0$, $X_0\simeq 0.028$, which is essentially the same value as above.

We now try to find the transition point X_0 analytically, i.e., as a series in ϵ. We assume that X_0 is of order ϵ; then one point of intersection of the boundary by the curve of zero velocity has x of order ϵ. We set

$$X_0=\rho_0\epsilon, \quad x=c\epsilon$$

and $X=Y=0$, $x_0=y_0=0$, and retain all the necessary terms up to the order ϵ^4. Then $Y_0^2=2h-X_0^2$,

$$Ay^2=(2h-Ax^2)\left(1+\frac{2\epsilon x}{A}+\frac{4\epsilon^2x^2}{A^2}\right),$$

and φ is written

$$Ax^2(2h-Ax^2)\left(1+\frac{2\epsilon x}{A}\right)-\frac{A^2x^4}{3}+\frac{(2h-Ax^2)^2}{12}\left(1+\frac{2\epsilon x}{A}+\frac{4\epsilon^2x^2}{A^2}\right)^2-X_0^2(2h-X_0^2)+\frac{X_0^4}{3}-\frac{(2h-X_0^2)^2}{12}$$
$$-\frac{2\epsilon}{9A}\left\{4x(2h-Ax^2)^2\left(1+\frac{2\epsilon x}{A}\right)^2+8hAx^3\right\}+\epsilon^2\left\{R_{06}(2h-Ax^2)^3\left(1+\frac{2\epsilon x}{A}\right)^3-S_{06}(2h-X_0^2)^3\right.$$
$$\left.+R_{24}Ax^2(2h)^2-S_{24}X_0^2(2h)^2\right\}+\epsilon^3R_{16}(A^{\frac{1}{2}}x)(2h)^3+\epsilon^4(R_{08}-S_{08})(2h)^4=0, \tag{72}$$

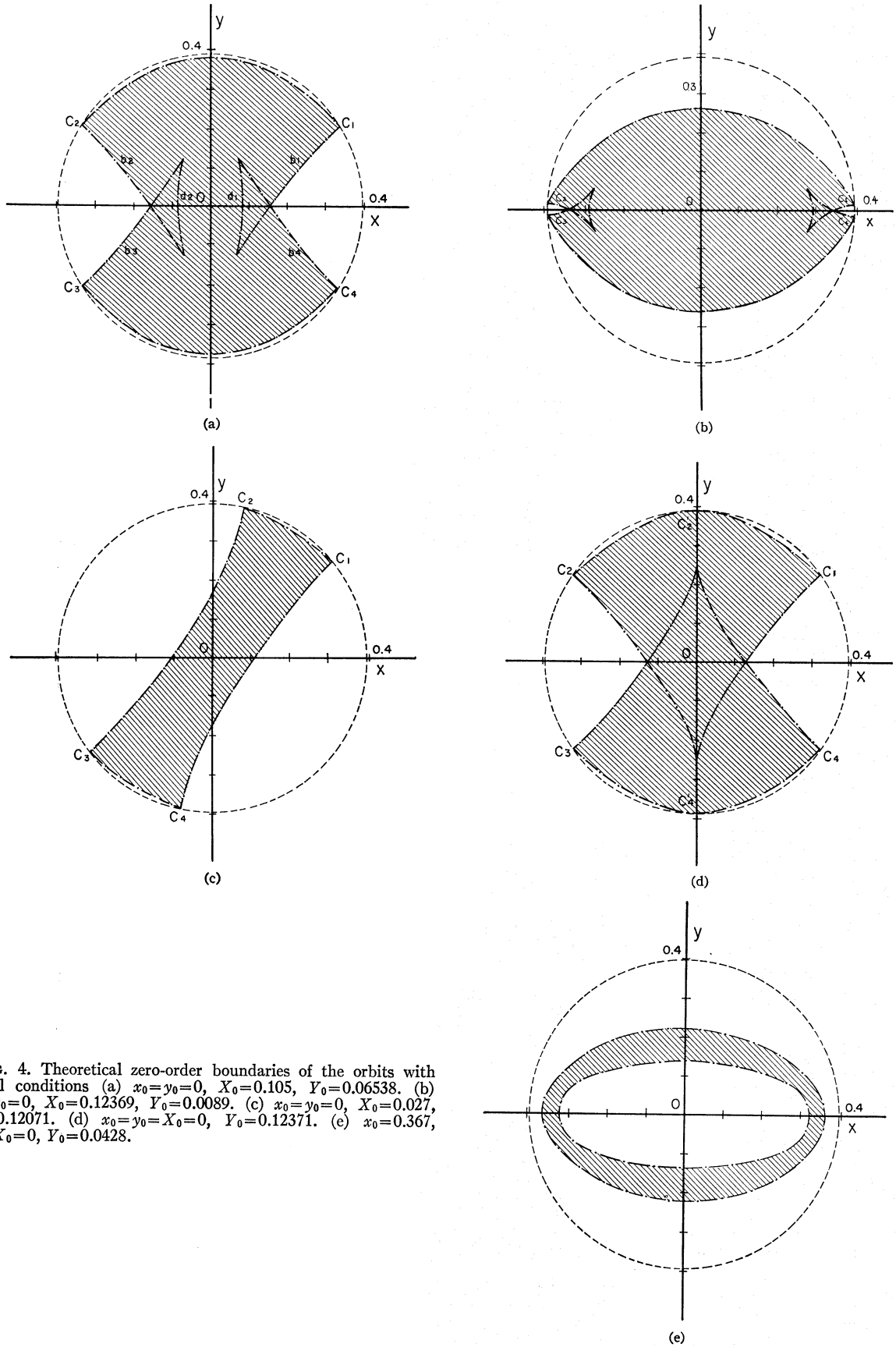

FIG. 4. Theoretical zero-order boundaries of the orbits with initial conditions (a) $x_0=y_0=0$, $X_0=0.105$, $Y_0=0.06538$. (b) $x_0=y_0=0$, $X_0=0.12369$, $Y_0=0.0089$. (c) $x_0=y_0=0$, $X_0=0.027$, $Y_0=0.12071$. (d) $x_0=y_0=X_0=0$, $Y_0=0.12371$. (e) $x_0=0.367$, $y_0=X_0=0$, $Y_0=0.0428$.

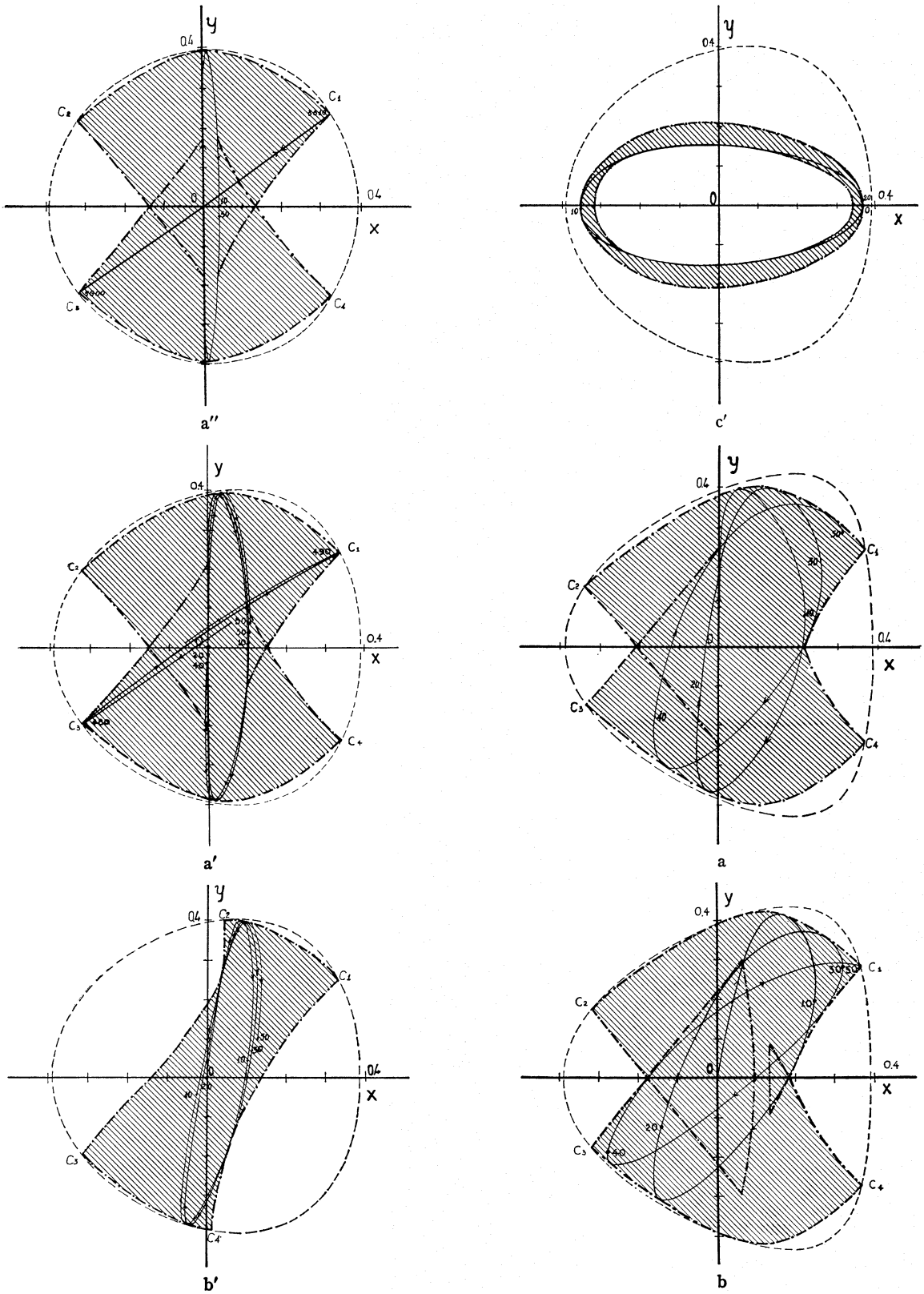

FIG. 5. Orbits for $A=0.1$ and (a'') $x_0=y_0=X_0=0$, $Y_0=0.12370$ ($\epsilon=0.02$). (a') $x_0=y_0=X_0=0$, $Y_0=0.12370$ ($\epsilon=0.05$). (b') $x_0=y_0=0$, $X_0=0.018$, $Y_0=0.1223765$ ($\epsilon=0.05$). (c') $x_0=0.367$, $y_0=X_0=0$, $Y_0=0.04280$ ($\epsilon=0.05$) (a) $x_0=y_0=X_0=0$, $Y_0=0.12370$ ($\epsilon=0.1$). (b) $x_0=y_0=0$, $X_0=0.026$, $Y_0=0.12093$ ($\epsilon=0.1$). (c) $x_0=y_0=0$, $X_0=0.027$, $Y_0=0.12071$ ($\epsilon=0.1$). (d) $x_0=y_0=0$, $X_0=0.070$, $Y_0=0.10198$

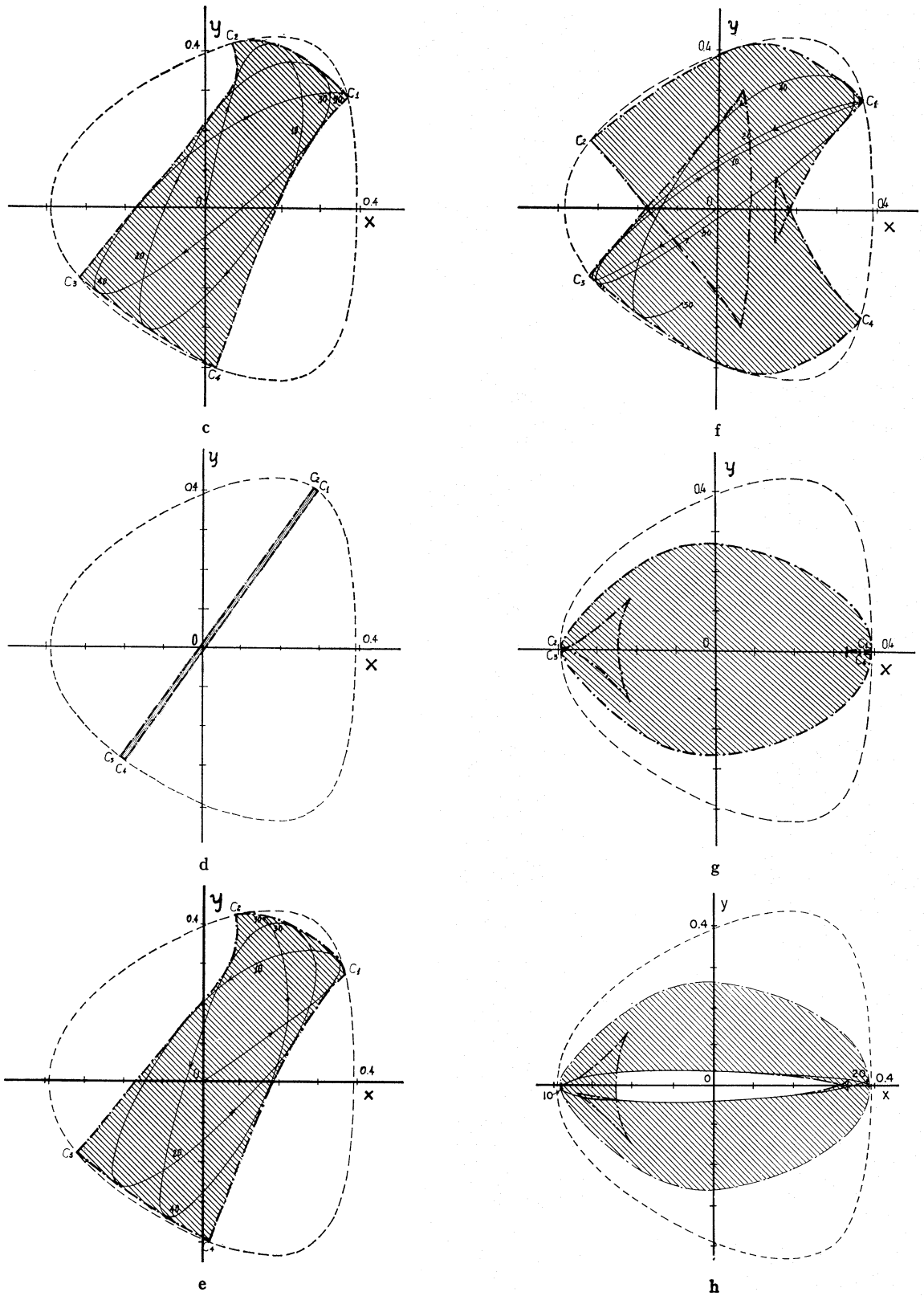

(ϵ=0.1). (e) $x_0=y_0=0$, $X_0=0.102$, $Y_0=0.06997$ (ϵ=0.1). (f) $x_0=y_0=0$, $X_0=0.103$, $Y_0=0.068491$ (ϵ=0.1). (g) $x_0=y_0=0$, $X_0=0.12369$, $Y_0=0.00089$ (ϵ=0.1). (h) $x_0=0.390$, $y_0=X_0=0$, $Y_0=0.009441$ (ϵ=0.1). The dashed-dotted lines represent the boundaries of the orbits. The dashed lines represent the curves of zero velocity.

where R_{06}, S_{06}, R_{24}, S_{24}, R_{16}, R_{08}, S_{08} are the coefficients of $(A^{\frac{1}{2}}y)^6$, Y^6, $(A^{\frac{1}{2}}x)^2(A^{\frac{1}{2}}y)^4$, $(A^{\frac{1}{2}}x)(A^{\frac{1}{2}}y)^6$, $(A^{\frac{1}{2}}y)^8$, Y^8 in φ_2, φ_3, φ_4, as given above. Then we find

$$c^2-\frac{4hc}{3A^2}-\frac{\rho_0^2}{A}+\frac{24h^2(R_{06}-S_{06})}{5A}+\epsilon^2\left[-\frac{3Ac^4}{4h}+\frac{8c^3}{3A}-\frac{92hc^2}{15A^3}+\frac{3\rho_0^4}{4hA}-\frac{36h}{5}\left(c^2R_{06}-\frac{4hcR_{06}}{A^2}-\frac{\rho_0^2S_{06}}{A}\right)\right.$$

$$\left.+\frac{12h}{5}\left(c^2R_{24}-\frac{\rho_0^2S_{24}}{A}\right)+\frac{24h^2cR_{16}}{5A^{\frac{1}{2}}}+\frac{48h^3}{5A}(R_{08}-S_{08})\right]=0. \quad (73)$$

This equation in zero-order approximation has real roots if

$$\rho_0^2\geqslant\frac{4h^2}{45A^3}[-5+54A^3(R_{06}-S_{06})]=\rho_1^2. \quad (74)$$

For $2h=0.0153$, $A=0.1$, we have $R_{06}-S_{06}=11/18A^3=611.111$ and we find a double root $c=2h/3A^2=0.51$ for $\rho_1^2=112h^2/45A^3=0.1457$ ($\rho_1\simeq 0.38$). If we set now $c=2h/3A^2+\epsilon\omega$ and

$$\rho_0^2=\rho_1^2+\epsilon^2R_0, \quad (75)$$

we find that ω is real if

$$R_0\geqslant\frac{8h^3}{27A^6}\left[\frac{1297}{150}+54A^3R_{06}+\frac{1512A^3S_{06}}{25}+\frac{18A^3R_{24}}{5}\right.$$

$$\left.-\frac{504A^3S_{24}}{25}+\frac{54A^{4\frac{1}{2}}R_{16}}{5}+\frac{162A^6}{5}(R_{08}-S_{08})\right]=R_1, \quad (76)$$

hence we have real roots (case B) only if

$$\rho_0^2\geqslant\rho_1^2+\epsilon^2R_1=\rho_2^2. \quad (77)$$

If $\bar{c}_3$, d_2 are not zero, and we include the terms $\frac{1}{3}\bar{c}_3(2H_0)^3+d_2(2H_0)\varphi_0$ in φ_2 we find

$$R_{06}=-903.54938+\tfrac{1}{3}\bar{c}_3+\tfrac{1}{12}d_2,$$

$$S_{06}=-1514.66049+\tfrac{1}{3}\bar{c}_3+\tfrac{1}{12}d_2,$$

$$R_{24}=-1230.32407+\bar{c}_3+\tfrac{1}{12}(13d_2),$$

$$S_{24}=325.23148+\bar{c}_3+\tfrac{1}{12}(13d_2),$$

and if we calculate also the terms of degree 7 and 8

$$R_{16}=177707.31635-(2\bar{c}_3/A^{1\frac{1}{2}})-(19d_2/18A^{1\frac{1}{2}}).$$

$$R_{08}-S_{08}=-549614.19753+(11d_2/18A^3).$$

Hence $R_1\simeq -13.2$.

This is independent of $\bar{c}_3$ and d_2 as it should be expected. Then for $\epsilon=0.05$ we find $\epsilon\rho_1=0.019$, and $\epsilon\rho_2=0.017$, for $\epsilon=0.1$, $\epsilon\rho_1=0.038$, and $\epsilon\rho_2=0.012$.

In the calculated orbits we have a transition from case A to case B between $X_0=0.0170$ and $X_0=0.0172$ for $\epsilon=0.05$ and between $X_0=0.026$ and $X_0=0.027$ for $\epsilon=0.1$. Therefore the formula (77) is satisfactory in the case $\epsilon=0.05$, but not in the case $\epsilon=0.1$. On the other hand, we have seen that the equation $\varphi_0=\varphi_{;0}$, truncated after $\epsilon^4\varphi_4$, gives satisfactorily the point of transition. Therefore the solution of the third integral equation is much better effected numerically in the case $\epsilon=0.1$ than by means of a truncated series. This result could not be predicted *a priori*. In general finding the accuracy of the results of a certain truncated series for different values of ϵ is a matter of experience. In this case it is quite insufficient to truncate the third integral after $\epsilon\varphi_1$, even for $\epsilon=0.05$, and we must include terms up to $\epsilon^4\varphi_4$ when $\epsilon=0.1$ (and then find the accurate numerical solution, and not a series expansion).

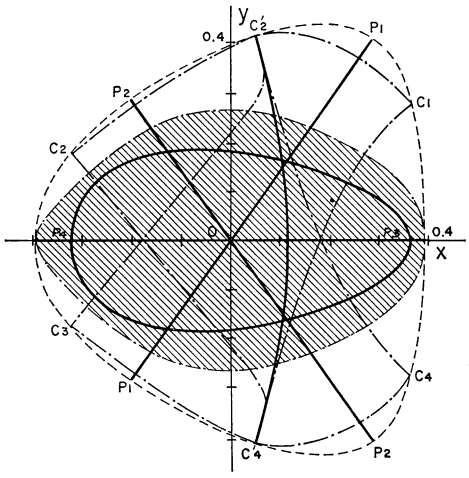

FIG. 6. Periodic orbits and limiting orbits for $A=0.1$, $2h=0.0153$ and $\epsilon=0.1$. The orbits P_1P_1, P_2P_2 and P_3P_4 are stable periodic orbits, and the x axis and $C_2'C_4'$ unstable periodic orbits. The limiting orbit between A- and B-type orbits is $C_1C_2C_3C_4$ and the limiting orbit between A- and C-type orbits is shaded.

B. Section with the x Axis (if $XY\neq 0$)

If $y=y_0=0$, Eq. (47) gives

$$15Y^4-2C_2Y^2+C_3=0, \quad (78)$$

and Eq. (50) gives $XY(-15Y^2+C_2)=0$. If we assume $XY\neq 0$, then

$$Y^2=C_2/15, \quad (79)$$

and Eq. (78) becomes

$$C_2^2-15C_3=0, \quad (80)$$

or

$$D(Ax^2)=144A^2x^4-480hAx^2+160h^2-180\varphi_{0;0}=0. \quad (81)$$

The roots are imaginary if $16h^2+12\varphi_{0;0}<0$ (case C).

In cases A, B the roots are real and their mean is $5h/3$. Further

$$D(0)=25(Y_0^2-2X_0^2)^2 + 20Ax_0^2(5Ax_0^2+10X_0^2+13Y_0^2)\geqslant 0. \quad (82)$$

Therefore there is only one root acceptable. This is zero if $x_0=0$ and $Y_0=\pm\sqrt{2}X_0$, i.e., for the straight line periodic orbits found above.

Thus the boundaries of the A- and B-type orbits have two angular points on the x axis, symmetric with respect to the origin in zero-order approximation. This is clearly seen in the calculated orbits. Only for orbits near the C type (i.e., with large initial x_0 and/or X_0) the angular point to the right does not appear (cf. Sec. IV).

C. Branch Perpendicular to the x Axis ($X=0$)

If $X=0$ Eq. (50) has three solutions:

(i) $x=0$; then we have a periodic motion along the y axis.

(ii) $Y^2=\frac{1}{2}C_1$. Then, because of Eq. (45) we have $C_1=0$, i.e., points on the curve of zero velocity.

(iii) $y=0$. Then Eqs. (45) and (47) give

$$15C_1^2-2C_2C_1+C_3=0, \quad (83)$$

or

$$E(Ax^2)=9A^2x^4-28hAx^2+4h^2-12\varphi_{0;0}=0. \quad (84)$$

The roots of this equation are real because the discriminant is

$$640h^2+432\varphi_{0;0}=4[(2X_0^2-7Ay_0^2)^2+(2Ax_0^2-7Y_0^2)^2 + 188(X_0Y_0+Ax_0y_0)^2+2A(2x_0X_0+7y_0Y_0)^2]\geqslant 0. \quad (85)$$

The roots must be between 0 and $2h$. We have

$$E(0)=4h^2-12\varphi_{0;0}=-\theta(0,0), \quad (86)$$

$$E(2h)=-16h^2-12\varphi_{0;0}=-\theta(0,2h), \quad (87)$$

and the mean of the roots is $14h/9$. Hence in case A one root is acceptable, in case B no root is acceptable, and in case C two roots are acceptable.

In the last case the two roots coincide if

$$Y_0=\pm x_0(2A/7)^{\frac{1}{2}} \quad \text{and} \quad X_0=\pm y_0(7A/2)^{\frac{1}{2}}. \quad (88)$$

The locus of these points on the x_0, y_0 plane is the ellipse

$$\frac{Ax_0^2}{7}+\frac{Ay_0^2}{2}=\frac{2h}{9} \quad (89)$$

and represents a (stable) periodic orbit.

If $y_0=X_0=0$, then Eq. (84) is written

$$9A^2(x^4-x_0^4)-28hA(x^2-x_0^2)=0,$$

i.e., the roots are

$$Ax^2=Ax_0^2 \quad \text{and} \quad Ax^2=-Ax_0^2+28h/9. \quad (90)$$

In case C the last quantity is between $10h/9$ and $2h$, because $10h/9<Ax_0^2<2h$. In case A only the first root is acceptable. Case B is impossible if $y_0=X_0=0$.

The transition between A- and C-type orbits occurs when $Ax_0^2\to 10h/9$, or $Ax_0^2\to 2h$. Then the solutions of Eq. (84) are $Ax^2\simeq 10h/9$ and $Ax^2\simeq 2h$. The inner boundary is reduced to a straight line segment between $x=-(10h/9A)^{\frac{1}{2}}$ and $x=(10h/9A)^{\frac{1}{2}}$, while the outer boundary is tangent to the curve of zero velocity at $x=\pm(2h/A)^{\frac{1}{2}}$.

In order to find the transition in higher approximation we set $y=y_0=X=X_0=0$ and $Ax^2=2h$, $Y^2=0$ in equation $\varphi-\varphi_{;0}=0$, truncated after $\epsilon^2\varphi_2$.

The terms different from zero are

$$-\frac{A^2x^4}{3}+Ax_0^2Y_0^2+\frac{A^2x_0^4}{3}-\frac{Y_0^4}{12}+\frac{2\epsilon}{A}(2Ax_0^3Y_0^2-7x_0Y_0^4) + \epsilon^2[-72.530864(A^3x^6-A^3x_0^6)+1514.660494Y_0^6 - 2269.675926Ax_0^2Y_0^4-430.555556A^2x_0^4Y_0^2]=0. \quad (91)$$

Then we may write

$$x_0=\pm(10h/9A)^{\frac{1}{2}}+\epsilon\omega_1+\epsilon^2\omega_2, \quad (92)$$

and to a second-order approximation

$$Ax_0^2=\frac{10h}{9}+2A\epsilon\left(\frac{10h}{9A}\right)^{\frac{1}{2}}\omega_1+A\epsilon^2\left[\omega_1^2+2\left(\frac{10h}{9A}\right)^{\frac{1}{2}}\omega_2\right], \quad (93)$$

and $Y_0^2=2h-Ax_0^2$.

After some operations we find

$$\omega_1=16h/27A^2, \quad (94)$$

and

$$\omega_2=\mp(41h^2/243A^4)(9A/10h)^{\frac{1}{2}}. \quad (95)$$

For $h=0.00765$ and $A=0.1$ we have in zero-order $x_0=\pm 0.29155$, and $\omega_1=0.4533$, $\omega_2=\mp 0.3387$.

The transition between A- and C-type orbits in first-order approximation is at $x=+0.314$ or -0.269 for $\epsilon=0.05$ and at $x=+0.337$ or -0.246 for $\epsilon=0.1$. In second-order approximation it is at $x=+0.313$ or -0.268 for $\epsilon=0.05$ and at $x=+0.3335$ or $x=-0.268$ for $\epsilon=0.1$. The actual transition has been found at $x\simeq 0.313$ for $\epsilon=0.05$ and at $x\simeq 0.333$ for $\epsilon=0.1$. The agreement is very good. The transition orbit is the unstable orbit $y=Y=0$. The limit of an orbit whose initial conditions are very near $y=Y=0$ is given in Fig. 6.

We proceed now to the calculation of the periodic orbit of type C in second-order approximation. If we set $y=X=y_0=X_0=0$,

$$x=x_0=\pm(14h/9A)^{\frac{1}{2}}+\epsilon\psi_1+\epsilon^2\psi_2 \quad (96)$$

and

$$Y^2=Y_0^2=2h-Ax^2, \quad (97)$$

we require that the solution $x=x_0$ be double, i.e.,

$$12(d\varphi/dx)_0=0. \quad (98)$$

We have $12(\varphi_0-\varphi_{0;0})=E(Ax^2)$; hence

$$12(d\varphi_0/dx)_0=36A^2x_0^3-56hAx_0. \quad (99)$$

In Eq. (22) only the terms $2Ax^3Y^2$ and $-7xY^4$ in φ_1 are different from zero, hence

$$12(d\varphi_1/dx)_0 = -(8/3A)(-45A^2x_0^4+96hAx_0^2-28h^2). \quad (100)$$

We have further

$$\varphi_2=-1514.660494Y^6+2269.675926Ax^2Y^4 +430.555556A^2x^4Y^2-72.530864A^3x^6,$$

hence

$$12\left(\frac{d\varphi_2}{dx}\right)_0=236250A^3x_0^5-830666.6667hA^2x_0^3 +654111.1111h^2Ax_0. \quad (101)$$

If we insert the value (96) we find after some operations

$$\psi_1=8h/27A^2, \quad (102)$$

and

$$\psi_2=\mp(64h/567A^3)(14h/9A)^{\frac{1}{2}}. \quad (103)$$

If $2h=0.0153$, $A=0.1$, we have $(14h/9A)^{\frac{1}{2}}=0.34496$, and $\psi_1=0.2267$, $\psi_2=\mp0.298$. Hence for $\epsilon=0.02$ we have $x_0=0.349$ and -0.340, for $\epsilon=0.05$, $x_0=0.356$ and -0.333 and for $\epsilon=0.1$, $x_0=0.365$ and -0.319.

The actual periodic orbit for $\epsilon=0.05$ is at $x_0=0.356$ ($y_0=X_0=0$, $Y_0=0.0512484$). The second point of intersection with the x axis is at $x=-0.334$. For $\epsilon=0.1$ the periodic orbit is at $x_0=0.364$ ($x_0=X_0=0$, $Y_0=0.0452813$, Fig. 6). The second point of intersection is at $x=-0.320$. The agreement is very good.

Equation (84) has also another double solution, for $x=x_0=0$. If we set $x=x_0=\epsilon\bar{\psi}_1+\epsilon^2\bar{\psi}_2+\epsilon^3\bar{\psi}_3$, $y=Y=y_0=Y_0=0$, in $12(d\varphi/dx)_0=0$, retaining only terms up to the third degree in ϵ, we find

$$-56hA(\epsilon\bar{\psi}_1+\epsilon^2\bar{\psi}_2+\epsilon^3\bar{\psi}_3)+36A^2\epsilon^3\bar{\psi}_1^3 -(8\epsilon/3A)(-28h^2+96hA\epsilon^2\bar{\psi}_1^2)+654111.1111h^2A\epsilon^3\bar{\psi}_1 -(10338.4/27A^4)h^2\epsilon^3=0, \quad (104)$$

the last term resulting from $12\epsilon^3(d\varphi_3/dx)_0$.

Hence

$$\bar{\psi}_1=4h/3A^2, \quad \bar{\psi}_2=0, \quad \bar{\psi}_3=32h^2/15A^5. \quad (105)$$

The first-order periodic orbit $x_0=\epsilon\bar{\psi}_1$ is the same as in the general irrational case (Contopoulos 1965).

For $2h=0.0153$, $A=0.1$ we have: $\bar{\psi}_1=1.02$, $\bar{\psi}_3=12.5$.

For $\epsilon=0.02$ we have a periodic orbit at $x_0=0.0205$. For $\epsilon=0.05$ the periodic orbit is at $x_0=0.0526$, and for $\epsilon=0.1$ it is at $x_0=0.1145$. In the last case the term $\epsilon^3\bar{\psi}_3$ is more than 10% of the term $\epsilon\bar{\psi}_1$.

The actual periodic orbits occur for $x_0=0.0526$ ($\epsilon=0.05$) and $x_0=0.116$ ($\epsilon=0.1$, Fig. 6), i.e., very near the theoretically calculated places, and they are unstable.

D. Section with the y Axis (if $XY\neq0$)

If $x=0$ Eqs. (47) and (50) give Eq. (80), which is now written

$$F(Ay^2)=144A^2y^4-240hAy^2+160h^2-180\varphi_{0;0}=0. \quad (106)$$

We have real solutions only if $-4h^2+12\varphi_{0;0}\geqslant0$ (case B).

Further, we must have $0\leqslant Ay^2\leqslant2h$ and $0\leqslant Y^2\leqslant2h-Ay^2$, where $Y^2=C_2/15=(20h-3Ay^2)/15$. These conditions are reduced to

$$0\leqslant Ay^2\leqslant5h/6.$$

But

$$F(0)=5(32h^2-36\varphi_{0;0})\geqslant0, \quad (107)$$

because of Eq. (60) and

$$F(5h/6)=15(4h^2-12\varphi_{0;0})\leqslant0. \quad (108)$$

Hence one root is always acceptable, i.e., in case B the boundary always intersects the y axis at an angle.

The limiting case $-4h^2+12\varphi_{0;0}=0$ happens for $Ay^2=5h/6$ and $Y^2=7h/6=2h-Ay^2$, hence $X^2=0$; this case has been considered already.

E. Branch Perpendicular to the y Axis ($Y=0$)

If $Y=0$ Eq. (50) has the following three solutions:

(i) $y=0$; then we have a periodic motion along the x axis.

(ii) $C_1=0$, i.e., points on the curve of zero velocity.

(iii) $x=0$. Then Eq. (47) gives

$$G(Ay^2)=9A^2y^4-8hAy^2-16h^2-12\varphi_{0;0}=0. \quad (109)$$

The discriminant of this equation is the same as that of Eq. (84). Therefore it is always positive, except for $Y_0=\pm x_0(2A/7)^{\frac{1}{2}}$, $X_0=\mp y_0(7A/2)^{\frac{1}{2}}$, (periodic orbit) when it is zero.

We have also

$$G(0)=-\theta(0,2h), \quad (110)$$

$$G(2h)=-\theta(0,0), \quad (111)$$

and the mean of the roots Ay^2 is $4h/9$.

Therefore in case B no root is acceptable. In case A one root is acceptable, and in case C both roots are acceptable.

In case C the periodic orbit intersects the y axis at the points $y=\pm(4h/9A)^{\frac{1}{2}}$. Thus the two roots of the general C case are on both sides of the double root of the periodic case. In fact it can be seen that the C-type orbits surround the periodic orbit.

If one root tends to zero, the other root tends to $Ay^2=8h/9$. This case is the transition case between A- and C-type orbits (Fig. 6). Therefore all orbits whose initial point is outside the boundary of the transition orbit are A- or B-type orbits.

IV. CALCULATED ORBITS

A large number of orbits have been calculated in the potential field (1) with $A=0.1$, $2h\simeq 0.0153$ (approximately), $\epsilon=0.1$, 0.05, and $\epsilon=0.02$, and different initial conditions. These values are of the same order as those used in paper I. Most calculations were made at the Goddard Institute for Space Studies, in double precision, by means of the Runge–Kutta method. The step used was 0.05 time units and the calculations were made usually for 400–600 time units. This interval was sufficient to give the general form of the orbits when $\epsilon=0.1$. When $\epsilon=0.05$ the calculations were extended, eventually, to 1200 time units. In case a″ it has been found necessary, in order to find the general form of the orbit, to go up to 5500 time units.

In all these cases the energy integral was conserved to eight significant figures (with an error 1 in the last figure in case a″, because the program was stopped many times and only eight significant figures were available for the continuation of the orbit). A check of the individual coordinates and velocities was made by repeating the calculations with a different step (0.02) in a few cases. The printed values were found accurate to seven significant figures, at least.

Some of the most characteristic orbits are represented in Fig. 5 (a″,a′,b′,c′a,b,c,d,e,f,g,h,).

All the orbits are contained inside the corresponding curves of zero velocity

$$A(x^2+y^2)-2\epsilon xy^2=2h, \tag{112}$$

which are drawn as dashed lines in Figs. 5.

This curve intersects the x and y axes at the points $\pm(2h/A)^{\frac{1}{2}}=\pm 0.391$. If $\epsilon=0$ the curve is a circle. The magnitude of the perturbation when $\epsilon\neq 0$ can be given by the maximum value of the ratio

$$\epsilon xy^2/h=\epsilon x(2h-Ax^2)/h(A-2\epsilon x), \tag{113}$$

which occurs when

$$4\epsilon x^3-3Ax^2+2h=0. \tag{114}$$

By solving this equation we find that $(\epsilon xy^2/h)_{\max}$ is 62%, 20%, and 7% for $\epsilon=0.1$, 0.05, and 0.02, respectively.

The maximum value of y on the curve on zero velocity occurs for x given by the equation

$$Ax^2-(A^2x/\epsilon)+2h=0. \tag{115}$$

The solution of this equation which is smaller than $(2h/A)^{\frac{1}{2}}$ is $x=0.189$, 0.080, and 0.031 for $\epsilon=0.1$, 0.05, and 0.02, respectively. The corresponding values of $y_{\max}$ are 0.435, 0.399, and 0.392.

The boundaries of the orbits are given in Fig. 5 as dashed-dotted lines. In some cases these lines are extended inwards, representing the tangents of sets of arcs of the orbits, which correspond to the branches b_1, b_2, b_3, b_4, d_1, d_2 of the theoretical boundaries [Fig. 4(a)]. The points where the arcs b_1, b_2, b_3, b_4 meet d_1, d_2 are not well defined.

It is noted that all boundaries, except those of type C, have four angular points on the curve of zero velocity.

The areas covered by the orbits are shaded. The initial arcs of the orbits (usually up to 50 time units) are also drawn in Figs. 5, as well as a few characteristic arcs.

Figures 5a, a′, a″ represent three orbits with the same initial velocity at the origin, going upwards ($x_0=y_0=Y_0=0$, $X_0=0.1237$) for three values of ϵ($\epsilon=0.1$, 0.05, 0.02). All three orbits are of type A; their boundaries remind of an hour glass. The moving point makes elongated loops clockwise with the long axes of the loops turning also clockwise. When the loop approaches the direction C_1C_3 the moving point begins to make loops counterclockwise and the axes of the loops turn also counterclockwise, until the loop approaches the direction C_2C_4, etc.

The loops are more elongated when ϵ is smaller, and the time needed to cover sparsely the area inside the boundary is much larger in this case. The first reversal of the sense of rotation occurs after about 90 time units when $\epsilon=0.01$, after 490 time units when $\epsilon=0.05$, and after 3600 time units when $\epsilon=0.02$. These results indicate that the time needed to fill the whole space may be proportional to $1/\epsilon^{2.5}$.

All orbits a, b, c, d, e, f, g, a′, b′, a″ have the same starting point and the same measure of initial velocity. Only the angles of this velocity with the x axis decrease progressively for the same value of ϵ, i.e., the projections X_0 of the initial velocities increase. The boundary of the A-type orbits is symmetric with respect to the x axis. It leaves four empty areas inside the curve of zero velocity, between every two of the angular points C_1, C_2, C_3, C_4. The empty areas between C_1 and C_2 and between C_3 and C_4 are small, except when the initial velocity makes a small angle with the x axis (case g); in the last case the empty spaces to the right and left are very small.

The inner "boundaries" form, in general, two triangles inside the area covered by the orbit. The triangle to the left is always larger than that to the right. As X_0 increases from 0 the two perpendicular inner branches approach each other. They coincide in the case of the unstable periodic orbit, which is perpendicular to the x axis (Fig. 6).

For larger values of X_0 we have B-type orbits. These orbits are asymmetric with respect to the axes. They surround the periodic orbit $y=x\sqrt{2}$; for this reason they are called "tube" orbits (Ollongren 1965). They also leave four empty areas inside the curve of zero velocity. If the initial velocity at the origin forms with the x axis an angle greater than $\tan^{-1}\sqrt{2}$ then the moving point forms initially clockwise loops, whose axes are turning clockwise until they approach the line C_1C_3. Then the moving point begins to describe counterclockwise loops

which turn also counterclockwise until they approach the line C_2C_4, etc. The behavior is similar to that of the orbits A, only the point C_2 is to the right of the point C_4, while in the case A it is to the left (and C_2, C_4 are, then, symmetric with respect to C_3, C_1). Figures 5(b), (c) represent orbits with $X_0=0.026$ and $X_0=0.027$. The two orbits are near each other for more than 100 time units but their general form is quite different.

If an orbit comes very near the unstable periodic orbit that separates the A- and B-type orbits, the moving point makes many narrow loops near the unstable periodic orbit, and then proceeds further across it (case A) or returns back (case B). Figure 4(b′) is a tube orbit ($X_0=0.018$, $\epsilon=0.05$), near the unstable periodic orbit. For $X_0=0.017$, $\epsilon=0.05$ we have an A-type orbit.

Figure 5(d) represents a tube orbit very near the periodic orbit. When the angle of the initial velocity with the x axis is larger than $\tan^{-1}\sqrt{2}$ the orbits are similar to those described above, only the loops are initially described counterclockwise. The boundary of orbit e [Fig. 5(e), $X_0=0.102$] is very similar to that of orbit c and the boundary of orbit f [Fig. 5(f), $X_0=0.103$] very similar to that of orbit b. The transition is the same unstable periodic orbit.

The orbit represented in Fig. 5(f) has initial velocity components $X_0=-0.103$, $Y_0=-0.068491$; it is the same with the orbit with $X_0=0.103$, $Y_0=0.068491$. It has also been checked that if two initial velocities are symmetric with respect to the axes, the boundaries of the orbits are the same, as expected.

For large X_0 [Fig. 5(g), $X_0=0.12369$] the orbit does not approach the periodic $y=Y=0$. This proves that the periodic orbit $y=Y=0$ is unstable.

In cases with large X_0 the inner triangle to the right is reduced to a point and then disappears. The vertical line, however, remains, and the boundary to the right does not have an angular point on the x axis.

These characteristics are explained by the distorted form of the invariant curves [Figs. 2(b) and 3]. For orbits of type B we never have $X=0$, i.e., the orbit never crosses perpendicularly the x axis. The orbits of type A always have two points for which $X=0$. The minimum value of x on the invariant curve (corresponding to two values $\pm X_1$) is always to the left of the left point where $X=0$; therefore the left boundary on the xy plane has an angular point on the x axis [$x=x_{\min}(y=0)$, $X=\pm X_1$], which is to the left of the left point $x(y=0, X=0)$. The invariant curves near the unstable invariant point show also a similar behavior to the right; the maximum x for $y=0$ is to the right of the right point $x(y=0, X=0)$, and a small triangle is formed by the boundary. However, for the outer invariant curves the maximum value of x occurs for $X=0$, therefore the outer boundary for $y=0$ is perpendicular to the x axis.

If $y_0=X_0=0$, and $x_0\neq 0$, but x_0 is smaller than a limiting value, we have an invariant curve intersecting the X axis, therefore the orbit is of type A, as described above.

If, however, x_0 is large enough, we have a C-type orbit [Figs. 5(h) ($\epsilon=0.1$) and 5(b′) ($\epsilon=0.05$)]. The C-type orbits surround a stable periodic orbit, that has the form of a distorted ellipse (Fig. 6). The C-type orbits are sometimes called "shell" orbits. Their boundary does not have any point in common with the curve of zero velocity. It is composed of two closed curves around the origin. For $\epsilon=0.1$ we see that the inner boundary forms sometimes (perhaps always) two triangles inside the ring filled by the orbit, symmetric with respect to the x axis, to the left of the y axis; thus the inner boundary has two angular points.

If $x_0>0$, $Y_0>0$, the invariant curve for $Y>0$ is a small closed curve to the right of the origin and for $Y<0$ a small closed curve to the left of the origin.

TABLE II. Characteristics of the orbits.

	x_0	y_0	X_0	Y_0	C_1	C_2	C_3	C_4	$x_{\min}$ $(y=0)$	$x_{\max}$ $(y=0)$	$x\binom{y=0}{X=0}$		$y(x=0)$	Type
a″	0.	0.	0.	0.12370	0.325 0.234	−0.318 −0.215			−0.135	+0.133	0	+0.041	±0.39	A
a′	0.	0.	0.	0.12370	+0.338 +0.243	−0.321 −0.194			−0.153	+0.150	0	0.103	±0.39	A
b′	0.	0.	0.018	0.1223765	0.333 0.252	0.044 0.398	−0.315 −0.202	0.007 0.393	−0.135	+0.139			+0.19 −0.39	B
c′	0.367	0.	0.	0.04280					−0.351 +0.343	+0.367 −0.314	−0.351 −0.314	+0.343 +0.367	±0.21 ±0.15	C
a	0.	0.	0.	0.12370	0.371 0.241	−0.338 0.152			−0.206	0.211	0	+0.211	±0.38	A
b	0.	0.	0.026	0.12093	0.359 0.280	−0.320 0.176			−0.174	0.180	+0.097	+0.133	±0.38	A
c	0.	0.	0.027	0.12071	0.360 0.281	0.071 0.415	−0.318 −0.178	0.027 −0.402	−0.173	0.178			+0.22 −0.39	B
d	0.	0.	0.070	0.10198	0.292 0.404	0.284 0.410	−0.206 −0.279	−0.195 −0.287	−0.010	0.007			±0.02	B
e	0.	0.	0.102	0.06997	0.363 0.282	0.081 0.418	−0.315 −0.018	0.017 −0.398	−0.160	0.175			+0.21 −0.39	B
f	0.	0.	0.103	0.068491	0.364 0.275	−0.321 0.175			−0.176	0.180	0.085	0.146	±0.39	A
g	0.	0.	0.12369	0.00089	0.391 0.0036	−0.391 0.0022			−0.375	0.332	−0.242	0.332	±0.26	A
h	0.390	0.	0.	0.009445					−0.388 +0.317	+0.390 −0.245	−0.388 −0.245	+0.390 +0.334	±0.04 ±0.26	C

When x_0 moves towards the curve of zero velocity, or inwards towards the limiting value separating the A- and C-type orbits the inner boundary becomes smaller and tends to disappear. The transition is the orbit generated by a slight perturbation of the unstable periodic orbit $y=Y=0$ (Fig. 6).

The general characteristics of the orbits represented in Fig. 5 are given in Table II. The values given in this table were found after the orbits were drawn, with the help of the numerical values of the coordinates and the velocities printed by the computer (these values are available by the author for any further use, as well as the Fortran program for the calculation of the orbits).

Table II gives the value of ϵ, the initial conditions of the orbit (the energy is always approximately 0.00765), the coordinates x, y of the angular points C_1, C_2, C_3, C_4, on the curve of zero velocity, with an accuracy ± 0.001 (in the case of A-type orbits C_3 and C_4 are symmetric with C_2, C_1), the values of $x_{\min}$ and $x_{\max}$ for $y=0$, the values of x when $y=0$, and when $X=0$ (perpendicular branches), the intersection of the boundary with the y axis, and the type of the orbit.

A comparison of these values with the theoretical solutions, to different orders of approximation, has been made. If only zero- or first-order approximation is used the deviations are large for $\epsilon=0.1$ and even for $\epsilon=0.05$.

For example, the formulas (70) and (71) give the following values for x_1 and x_2, to be compared with the values of Table II:

	x_1	x_2
a, a′, a″:	0	$\pm 0.319 (C_1,C_2)$
b:	± 0.082	$\pm 0.309 (C_1,C_2)$
c:	$\pm 0.085 (C_2,C_4)$	$\pm 0.308 (C_1,C_3)$
d:	$\pm 0.221 (C_2,C_4)$	$\pm 0.230 (C_1,C_3)$
e:	$\pm 0.323 (C_1,C_3)$	$0 \quad (C_2,C_4)$
f:	$\pm 0.326 (C_1,C_2)$	
g:	$\pm 0.391 (C_1,C_2)$	
b′:	$\pm 0.057 (C_2,C_4)$	$\pm 0.314 (C_1,C_2)$

If we solve the Eqs. (8) and (44) in first order we find

$$x_i = x_{i0} + (\epsilon y_i^2/3A),$$

where x_{i0} is the corresponding zero-order solution.

The values of x_2 for the cases a, a′, a″ are now (0.336, −0.302), (0.328, −0.311), (0.323, −0.316). The last values compare rather satisfactorily with the empirical values (0.325, −0.318).

A second-order approximation was also calculated in some cases. The results are then closer to the empirical ones, but not accurate enough. For example, in case e the point C_1 in zero, first and second approximation is at $x=0.323$, 0.339, and 0.354, while the empirical value is 0.363. The difference is due to the fact that only after the inclusion of terms up to $\epsilon^4\varphi_4$ one can expect a fair agreement between theoretical and experimental results, and even then the numerical solution of the equations gives better results than the use of series expansions, as we have seen in Sec. IIIA. Zero- and first-order results are useful only for very small ϵ (e.g., $\epsilon=0.02$). For this reason although first-order and, eventually, second-order formulas have been developed to give the characteristic points of the boundaries, they have not been included, in general, in this paper.

For practical purposes it is sufficient to solve the equations numerically, by means of a computer.

A numerical solution of the equations to fourth-order approximation gives for C_1, C_2 in case a: $x=0.374$, -0.342, and in case b: $x=0.366$, -0.322, in fair agreement with the values of Table I. This, together with the fact that the empirical invariant curves are very near to the fourth-order theoretical invariant curves proves that the third integral can describe quantitatively, and not only qualitatively, the main characteristics of the calculated orbits.

V. CONCLUSIONS

The case $A=B$ is the most characteristic resonance case, when the two unperturbed frequencies along the axes x and y are equal. As the potential (1) is the most simple nonseparable potential, it provides a good occasion to study the resonance phenomena in detail.

It is known that in the other resonance cases (except if $A^{\frac{1}{2}}/B^{\frac{1}{2}}=2$) the forms of the orbits are in general boxes similar to those of the nonresonance cases (paper I). In the present case, however, we do not have any box type orbits at all. The A-type orbits have essential differences from the box-type orbits (angular points of the boundaries on the x axis, inner boundaries, different invariant curves).

It is remarkable, therefore, that even in this case the third integral is applicable with success. Although the use of only a few terms of the third integral did not give satisfactory numerical results in the case $\epsilon=0.1$ (because this value is near the escape case $\epsilon=0.118$, when the curves of zero velocity open and the moving point may escape to infinity), the inclusion of some higher-order terms gave a good agreement between theory and numerical experiments.

A complete discussion of more general potentials must include both a theoretical discussion of the form of the third integral and a comparison with numerical experiments. The following remarks should be made in this connection.

(a) As a first step numerical experiments are needed to indicate the possible existence of an isolating or nearly isolating third integral.

(b) The third integral can be usually developed in the form of a series. This series may be rather different from that of the nonresonance cases. The constancy of this integral should be checked for some orbits. In this way one will find how many terms of the third integral are needed to secure a sufficient accuracy. It is remarkable that an increase of the number of

terms has given always better results in all the cases we have considered, although one might expect the contrary, on the assumption that the third integral is not convergent but only an asymptotic expansion. It should be useful, however, to extend such calculations to cases where the dissolution of the invariant curves indicates that the third integral is not isolating, but only quasi-isolating.

(c) The first terms of the third integral can be used to find the form of the invariant curves for all the initial conditions inside the curve of zero velocity. This gives an immediate classification of the totality of the orbits. Otherwise, just calculating many orbits is a very slow process as regards their classification.

(d) If the theoretical invariant curves deviate from the computed ones, further terms of the third integral should be taken into account.

(e) The general forms of the orbits and their boundaries can also be found by means of the third integral and be compared to the actually calculated orbits. A more careful analysis will give finally the periodic orbits and the transition orbits.

(f) One further step would be the discussion of the third integral and of the forms of the orbits for increasing values of the perturbation, until the integral ceases to be isolating (or very nearly isolating). This has been done experimentally in the case of the potential (1) by Barbanis (1965). A comparison of such an analysis with an application of the third integral, when higher-order terms are included, may indicate why and how the third integral becomes quasi-isolating, and eventually, ergodic.

(g) Although a different form of the third integral may be used near each periodic orbit, it is remarkable that, in our case at least, the same formula is applicable for all kinds of orbits, up the the limiting curve ($Ax^2+X^2=2h$). As Barbanis (1965) has found, the dissolution of the invariant curves begins not near the limiting curve, but near the unstable periodic orbit which is perpendicular to the x axis. The C-type orbits are very nearly isolating, even when the curves of zero velocity become open and all the other orbits escape to infinity. This result may be compared to our result that the third integral is much better conserved in the case of the C-type orbits.

The conclusion is that the third integral is not local, in the sense that it is valid only near the origin, but represents the totality of the orbits.

VI. APPLICATIONS

A. Formula (1) may represent roughly the potential field on the plane of symmetry of a galaxy that has been deformed by interaction with another galaxy, so that it does not have an axis of symmetry. Of course, in practice the potential will contain many more terms, and, eventually, will not have an axis of symmetry on the plane xy, or even a plane of symmetry. However, it is useful to look at the potential (1) from the point of view of a distorted galaxy. Then a comparison with an axially symmetric galaxy gives the following results:

(a) If a point is ejected from the center, or a point near the center, in the case of circular symmetry it would be a straight line or a very elongated ellipse. In the present case it is a B-type orbit, filling a long strip, or an A-type orbit, which later may be near an open ellipse or a circle.

(b) If the initial velocity is perpendicular to the axis the orbit is nearly circular or elliptical (C-type orbit) only if the initial point is far away from the center. Most orbits, however, are of type A, i.e., if the moving point is rotating initially clockwise, after a long time its orbit will become almost rectilinear through the center and then it will reverse its direction of rotation.

By a convenient choice of the units of length and time we may fit the calculations of this paper to a model of a nearly spherical homogeneous galaxy, which has, at a distance of 10 kpc from the center, a circular velocity 250 km/sec.

In the unperturbed case ($\epsilon=0$) we have circular velocity Y_0 at a point x_0, ($y_0=X_0=0$) such that $Ax_0^2=Y_0^2=0.00765$, hence $x_0=0.2766$, $Y_0=0.08746$. If we set $x_0=10$ kpc$=0.2766L$ and $Y_0=250$ km/sec $=0.08746LT^{-1}$, where L, T are the units of length and time, we find

$$L=36.15 \text{ kpc}, \quad T=1.40\times10^7 \text{ yr}.$$

If $\epsilon=0.05$, i.e., if the maximum perturbation is $\sim20\%$, we need ~500–800 time units (7–11×10^9 yr) to change from an almost circular to an approximately rectilinear orbit, and ~1000–1500 time units (14–21×10^9 yr) to reach an almost circular motion in the opposite direction.

These times are long in comparison with the ages of the galaxies; they are small, however, in comparison with the relaxation times.

The limit between A- and C-type orbits occurs at about $x_0\simeq0.3$, i.e., $x_0\simeq11$ kpc. Therefore the initially circular orbits are A type, i.e., they do not remain almost circular except for a small time. Orbits with the same energy for $x_0>11$ kpc are C-type orbits. i.e., they are roughly elliptical orbits with a rotation of the apsides. The most distant point that can be reached by an orbit with this energy is $x=14$ kpc (rectilinear orbit).

If we assume circular orbits near the center of the galaxy, with $x_0\simeq3$ kpc and $Y_0\simeq200$ km/sec, we find $L\simeq11$ kpc and $T\simeq0.48\times10^7$ yr, i.e., the times necessary to transform an almost circular orbit into a rectilinear or a circular one in the reverse direction are 2–4×10^9 yr and 5–8×10^9 yr, respectively.

Therefore in the case of moderately distorted galaxies the times necessary to change appreciably the character of the circular orbits are of the order of the age of the galaxies or larger for the outer parts and smaller for the inner parts of the galaxies.

Similar results have been found recently for spiral galaxies by Barbanis. Such calculations are necessary in order to find the long-range behavior of the orbits of stars in a galaxy.

B. A second application of the above calculations is in the problem of the energy exchange between two coupled oscillators (see, e.g., Ford and Waters 1963). One may use the quantities $\Phi_{10}=\frac{1}{2}(Ax^2+X^2)$ and $\Phi_{20}=\frac{1}{2}(Ay^2+Y^2)$ to represent the energy in two directions. In the nonresonance cases these quantities are approximately conserved, if the perturbation ϵ is small. This is because $\Phi_1=\Phi_{10}+\epsilon\Phi_{11}+\cdots$ and $\Phi_2=\Phi_{20}+\epsilon\Phi_{21}+\cdots$ are integrals of motion. The same happens also in the general rational case (paper I), because we have in zero-order $\Phi_{10}+\Phi_{20}=h=\text{const}$, and

$$\varphi=\varphi_0\simeq c_1(2\Phi_{10})^2+c_2(2\Phi_{10})(2\Phi_{20})+c_3(2\Phi_{20})^2\simeq\text{const},$$

therefore approximately $\Phi_{10}\simeq\text{const}$, $\Phi_{20}\simeq\text{const}$.

In the present case, however, φ_0 has also the term C_0, therefore a separation of Φ_{10} and Φ_{20} is not possible. In fact, in the calculated orbits an appreciable exchange of energy between the two degrees of freedom x and y was observed.

We have taken a number of points on the orbits given in Fig. 5 and we calculated the mean values and the dispersions of the quantities $2\Phi_{10}$, $2\Phi_{20}$ and $2h-2\Phi_{10}-2\Phi_{20}$ in units 10^{-4}:

	$2\Phi_{10}$	$2\Phi_{20}$	$2h-2\Phi_{10}-2\Phi_{20}$
a″	18±18	58±19	0± 1
a′	23±20	55±20	− 1± 6
b′	21±20	56±19	− 1± 5
c′	60± 4	17± 4	− 3± 2
a	32±20	49±21	− 5±10
b	24±20	58±19	− 6±10
c	24±21	58±19	− 6±10
d	29± 6	58±13	−10±20
e	19±17	64±18	− 6±10
f	19±18	63±19	− 6±10
g	71±11	6±10	0± 3
h	57± 8	19± 7	+ 1± 3

It is seen that only in the cases d, h, and c′, i.e., near the stable periodic orbits the dispersions are comparatively small.

The third integral can give immediately the amount of energy exchange. The invariant curves (Figs. 1, 2, and 3) give the variation of the quantity $2\Phi_{10}$ at the points $y=0$. If R and r are the maximum and minimum distances of the invariant curve from the origin, then $2\Phi_{10\,\max}(y=0)=R^2$ and $2\Phi_{10\,\min}(y=0)=r^2$.

We will find these values in zero order. For a type A orbit the maximum $2\Phi_{10}$ occurs at the X axis; it is the solution of equation

$$\theta(0,X^2)=0, \qquad (116)$$

[cf. Eq. (31)]. The minimum ($2\Phi_{10}$) occurs at the $A^{\frac{1}{2}}x$ axis; it is the solution of the Eq. (33). For example if $r=0$ ($x_0=y_0=X_0=0$), the invariant curve intersects the X axis for $X^2=4h/3$. Therefore $2\Phi_{10\,\max}(y=0)=4h/3$ and $2\Phi_{10\,\min}(y=0)=0$. In the other A cases $2\Phi_{10\,\max}$ is a little larger, but $2\Phi_{10\,\min}$ is also larger. This means that we do not have complete exchange of energy between the directions x and y. In the case of a type B orbit the maximum and minimum $2\Phi_{10}$ for $y=0$ are the two solutions of the Eq. (116). In a type C orbit they are the two solutions of Eq. (33). When an orbit is near a stable periodic orbit the exchange of energy between the two degrees of freedom is small. For example, in the case of the orbits P_1, P_2 it is zero. The same is the case along the orbit P_3, P_4 because then $Ay^2+Y^2=(2/7)(X^2+Ax^2)=4h/9$.

A more detailed analysis can give the energy transfer when ϵ is not very small and $y\neq 0$ also. Thus the third integral can explain quantitatively the transfer of energy between two coupled oscillators. The appreciable exchange of energy observed in coupled systems under resonance conditions does not indicate the nonexistence of the third integral, but only that the third integral is not given by a formula $\Phi_1=\frac{1}{2}(Ax^2+X^2)+$higher-order terms.

[We would like to indicate a few typographical errors in paper I:

On p. 766 col. 2, lines 2 and 4 from below Φ should be replaced by φ; the same on p. 767 col. 1, lines 1 and 16; and in col. 2, lines 10 and 15 the first Φ_0 should be replaced by φ_0. On p. 768, col. 1, line 13 add a bar in S_2. On p. 769, col. 2, line 13 from below: $P=1.6$ (not $P=0.4$). In Eq. (47) z^4/Q should be replaced by $z^4/2$, and in Eq. (67) the quantity $(4Q\xi^2+3Qz^2-v_0^2)$, after ξ^4, should be squared.]

A great part of this research was done while one of us (G.C.) was a National Academy of Sciences–National Research Council senior research associate under the National Aeronautics and Space Administration. We wish to thank Dr. Robert Jastrow for the use of the computing facilities at the Institute for Space Studies. We thank also Dr. M. Davis for the use of the computer at Yale University and G. Bozis for help in the computer calculations. This work was supported by the Royal Hellenic Research Foundation.

REFERENCES

Barbanis, B. 1965, *Astron. J.* (to be published).
Contopoulos, G. 1960, *Z. Astrophys.* **49**, 273.
——. 1963, *Astron. J.* **68**, 763.
——. 1965, *ibid.* **70**, 526.
Ford, J., and Waters, J. 1963, *J. Math. Phys.* **4**, 1293.
Ollongren, A. 1965, *Ann. Rev. Astron. Astrophys.* **3**, 113.